4. Regional Environment

By Klaus J. Schulz

Volcanogenic Massive Sulfide Occurrence Model

Scientific Investigations Report 2010–5070–C

U.S. Department of the Interior
U.S. Geological Survey

U.S. Department of the Interior
KEN SALAZAR, Secretary

U.S. Geological Survey
Marcia K. McNutt, Director

U.S. Geological Survey, Reston, Virginia: 2012

For more information on the USGS—the Federal source for science about the Earth, its natural and living resources, natural hazards, and the environment, visit http://www.usgs.gov or call 1–888–ASK–USGS.

For an overview of USGS information products, including maps, imagery, and publications, visit http://www.usgs.gov/pubprod

To order this and other USGS information products, visit http://store.usgs.gov

Suggested citation:
Schulz, K.J., 2012, Regional environment in volcanogenic massive sulfide occurrence model: U.S. Geological Survey Scientific Investigations Report 2010–5070 –C, chap. 4, 24 p.

Contents

Geotectonic Environment....................37
Mid-Ocean Ridges and Mature Back-Arc Basins (Mafic-Ultramafic Lithologic Association)....................37
Sediment-Covered Ridges and Related Rifts (Siliciclastic-Mafic Lithologic Association)....................39
Intraoceanic Volcanic Arcs and Related Back-Arc Rifts (Bimodal-Mafic Lithologic Association)....................41
Continental Margin Arcs and Related Back-Arc Rifts (Bimodal-Felsic and Felsic-Siliciclastic Lithologic Associations)....................42
Temporal (Secular) Relations....................43
Duration of Magmatic-Hydrothermal System and Mineralizing Processes....................43
Relations to Structures....................45
Relations to Igneous Rocks....................49
Flow Lithofacies Association....................50
Volcaniclastic Lithofacies Association....................50
Relations to Sedimentary Rocks....................52
Relations to Metamorphic Rocks....................52
References Cited....................53

Figures

4–1. Schematic diagram showing volcanogenic massive sulfide deposits in divergent and convergent plate tectonic settings....................38
4–2. Schematic diagram showing proposed hydrothermal fluid flow at a fast-spreading ridge....................38
4–3. Structural map of the Gulf of California showing the extent of newly accreted oceanic crust in extensional basins along an extension of the East Pacific Rise....................40
4–4. Histograms showing number of volcanogenic massive sulfide deposits and contained metal of Cu+Zn+Pb in million tonnes....................44
4–5. Schematic diagram showing examples of the different structural settings of hydrothermal vents relative to faults and breakdown regions....................46
4–6. Model for fluid circulation and types of hydrothermal venting related to the development of detachment faults along slow-spreading mid-ocean ridges....................47
4–7. Conceptual diagram showing the evolution of a caldera-related submarine magmatic-hydrothermal system....................48
4–8. Composite stratigraphic sections illustrating flow, volcaniclastic, and sediment dominated lithofacies that host volcanogenic massive sulfide deposits....................51

4. Regional Environment

By Klaus J. Schulz

Geotectonic Environment

Volcanogenic massive sulfide (VMS) deposits are formed in marine tectonic settings where a strong spatial and temporal relationship exists between magmatism, seismicity, and high-temperature hydrothermal venting. These settings include extensional oceanic seafloor spreading ridges, volcanic arcs (oceanic and continental margin), and related back-arc basin environments (fig. 4–1). In addition, extensional environments may form in post-accretion and (or) successor arc settings (rifted continental margins and strike-slip basins). Volcanogenic massive sulfide deposits in Proterozoic and Phanerozoic sequences can generally be assigned to specific plate tectonic regimes, with all but the siliciclastic-felsic type represented by modern analogs (table 2–1). However, the assignment of deposits in Archean terranes is less certain, as the role of conventional plate tectonic systems in early earth history continues to be debated (Condie and Pease, 2008). Thus, although Archean VMS deposits can be classified by the relative amounts of associated mafic, felsic, and sedimentary rock, such classification does not necessarily correspond to modern plate tectonic settings. However, because plate tectonic processes appear to have operated at least since the Paleoproterozoic and possibly earlier, the geotectonic environments of VMS deposits are described below in the context of modern plate tectonic regimes.

In the modern oceans, the majority of known hydrothermal activity is located along mid-ocean ridges (65 percent), with the remainder in back-arc basins (22 percent), along volcanic arcs (12 percent), and on intraplate volcanoes (1 percent) (Baker and German, 2004; Hannington and others, 2004), but this distribution is likely biased by ridge-centric exploration driven by programs such as Ridge and InterRidge. In contrast, most VMS deposits preserved in the geologic record appear to have formed in extensional oceanic and continental volcanic arc and back-arc settings like the Miocene Japan arc–back-arc system and the modern Okinawa Trough and Lau and Manus Basins (Allen and others, 2002; Franklin and others, 2005). The general paucity in the geologic record of VMS deposits that formed on mid-ocean ridges likely reflects subduction and recycling of ocean floor crust since at least the Paleoproterozoic; the crust of the present ocean floor is no older than180 million years (m.y.).

Although VMS deposits formed on mid-ocean ridges are rarely preserved in the geologic record, study of the volcanic, tectonic, and hydrothermal processes occurring at modern ridge crests forms much of the basis for current models of VMS-forming hydrothermal systems (Hannington and others, 2005). High-temperature (350 °C) black smoker vents, first discovered on the East Pacific Rise in 1979 (Francheteau and others, 1979: Speiss and others, 1980), are the most recognizable features of seafloor hydrothermal activity and are most common on intermediate- to fast-spreading mid-ocean ridges. Studies of black smokers continue to provide important information on the geodynamic and chemical processes that lead to the formation of seafloor hydrothermal systems; however, because of their inaccessibility, important questions about their formation and evolution remain, including the three dimensional structure of seafloor hydrothermal systems and the source(s) of heat driving high-temperature fluid circulation. These aspects of VMS-forming systems, as well as the regional architecture of the volcanic sequences hosting deposits, are more easily investigated through detailed and regional-scale studies of ancient VMS environments (for example, Galley, 2003). However, interpretations of the setting of ancient VMS deposits can be difficult, particularly when they are present in tectonically deformed slivers in an orogen.

The tectonic settings described below represent end-member types; many natural settings are transitional in some respects between these settings (for example, a volcanic arc and related back-arc basin may change laterally from continental to oceanic).

Mid-Ocean Ridges and Mature Back-Arc Basins (Mafic-Ultramafic Lithologic Association)

The present global mid-ocean ridge system forms a submarine mountain range more than 50,000 kilometers (km) long and that averages about 3,000 meters (m) above the abyssal seafloor. Different types of ridges are discriminated on the basis of spreading rate and morphology, which vary in response to regional tectonic stresses and rates of magma supply (Sinha and Evans, 2004; Hannington and others, 2005). These factors also influence the size and vigor of hydrothermal convection systems on ridges, and there is a general positive correlation between increasing spreading rate and the

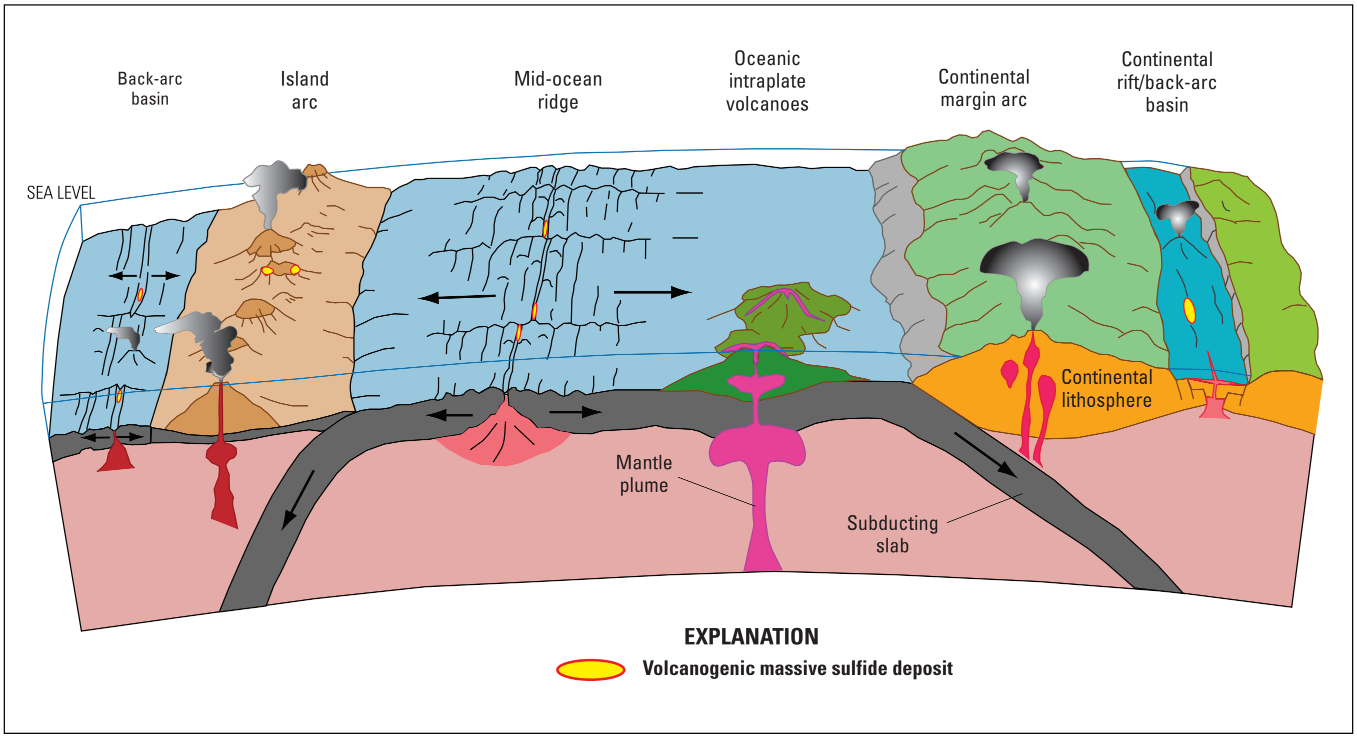

Figure 4–1. Schematic diagram showing volcanogenic massive sulfide deposits in divergent (mid-ocean ridge and back-arc basin) and convergent (subduction related island arc and continental margin arc) plate tectonic settings. Modified from Schmincke (2004) and Galley and others (2007).

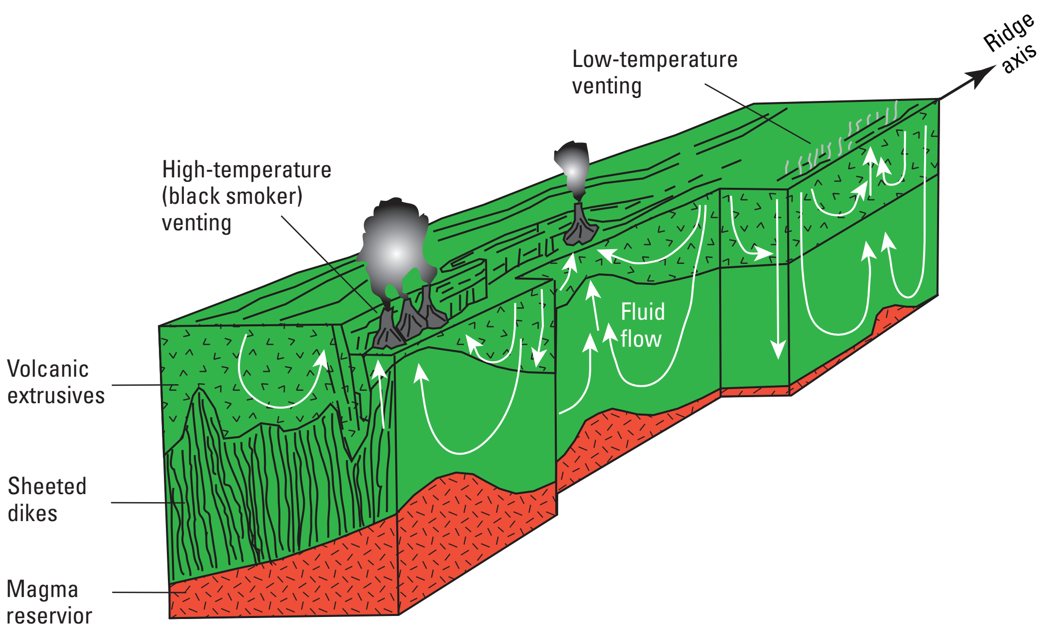

Figure 4–2. Schematic diagram showing proposed hydrothermal fluid flow at a fast-spreading ridge (for example, East Pacific Rise). Note that high-temperature (black smoker) vents occur above shallower segments of the axial magma reservoir. Modified from Haymon and others (1991).

incidence of hydrothermal venting (Baker and others, 1996; Baker, 2009).

At fast-spreading centers (full spreading rates of 6 to ≥10 centimeters per year [cm/yr]) such as the East Pacific Rise, high-temperature fluids circulate to relatively shallow depths (1–2 km) (fig. 4–2), owing to the intermittent presence of magma in shallow subaxial chambers, and venting correlates closely with the areas of most recent volcanic eruptions. However, the deposits formed on fast-spreading centers tend to be small (less than a few thousand tons) because frequent eruptions tend to disrupt the flow of hydrothermal fluids and bury sulfide accumulations, and because the vent complexes are rapidly displaced from their heat source by the fast spreading rate (Hannington and others, 2005). Intermediate-rate spreading centers (4–6 cm/yr), such as the Juan de Fuca and Gorda Ridge systems and the Galapagos Rift in the eastern Pacific Ocean, are characterized by lower rates of magma supply, deeper axial valleys, and greater structural control on hydrothermal fluid upflow than at fast-spreading ridges. Intermediate-rate spreading centers have some of the largest known vent fields, with venting commonly focused along the rift valley walls or in axial fissure zones. For example, the Endeavour segment of the Juan de Fuca Ridge has 50–100 black smokers located in six evenly spaced vent fields, 2–3 km apart, along a 15-km segment of the axial valley (Delaney and others, 1992; Kelley and others, 2001). Slow-spreading ridges (1–4 cm/yr) like the Mid-Atlantic Ridge between 13° and 15°N, are characterized by low rates of magma supply and only intermittent local eruptions of basalt. These ridges show evidence of vigorous tectonic extension characterized by large amounts of rotation on normal faults and exposures of intrusive gabbros and serpentinized ultramafic rocks in core complexes formed by detachment faulting (Escartin and others, 2008; Smith and others, 2008). At several locations along the Mid-Atlantic Ridge, black smokers and massive sulfide deposits, some characterized by enrichments in Ni, Co, and platinum group elements, occur on top of serpentinized ultramafic rocks representing exposed mantle (Krasnov and others, 1995; Bogdanov and others, 1997; McCaig and others, 2007). As shown by the TAG hydrothermal field on the Mid-Atlantic Ridge, large, long-lived hydrothermal systems can develop on slow-spreading ridges (Kleinrock and Humphris, 1996; Humphris and Tivey, 2000; Petersen and others, 2000).

Because ocean basins and their contained ridges compose more of the Earth's surface (approx. 48 percent) than any other crustal type, submarine volcanic rocks are the most widespread and abundant near-surface igneous rocks on Earth, and about 80 percent or more of these rocks are basalt generated at mid-ocean ridges. Basalts that form mid-ocean ridge crust (MORB) are dominantly subalkaline tholeiitic basalt characterized by depletions in thorium (Th), uranium (U), alkali metals, and light rare earth elements (NMORB; Viereck and others, 1989) relative to ocean island and continental basalts and have distinctive isotopic characteristics (Hofmann, 2003). Some intermediate- and slow-spreading centers have more evolved magma compositions (ferrobasalt and andesite) that reflect fractional crystallization, magma mixing, and (or) local crustal assimilation at shallow to intermediate depths (Perfit and others, 1999). In addition, some spreading centers (for example, portions of the Juan de Fuca Ridge system) also have enriched tholeiitic basalts (EMORB) with elevated concentrations of incompatible trace elements (for example, Ba, Cs [cesium], Rb [rubidium], Th, U, K [potassium], light rare earths); these enrichments also may be reflected in the composition of hydrothermal fluids and sulfide deposits at these locations (Hannington and others, 2005). Although most ancient ocean floor appears to have been subducted over time, rare obducted remnants, such as the Ordovician Bay of Islands ophiolite in Newfoundland (Bédard and Hébert, 1996), are present in some orogens. However, most ophiolites are fragments of extensional arc and back-arc basins formed in suprasubduction zone settings (Pearce, 2003). Although few ancient examples of VMS deposits formed on mid-ocean ridges are known, those formed at spreading centers in suprasubduction zone settings (mafic-ultramafic association) include deposits in the Troodos complex, Cyprus (for example, Mavrovouni deposit; Galley and Koski, 1999); the Oman ophiolite, Oman (for example, Lasail deposit; Alabaster and Pearce, 1985); the Løkken ophiolite in central Norway (for example, Løkken deposit; Grenne, 1989); the Betts Cove ophiolite, Newfoundland (for example, Betts Cove deposit; Sangster and others, 2007); and the Josephine ophiolite, Orogen (for example, Turner Albright deposit; Zierenberg and others, 1988).

Sediment-Covered Ridges and Related Rifts (Siliciclastic-Mafic Lithologic Association)

Active spreading centers that become proximal to continental margins through subduction of ocean crust (Juan de Fuca and Gorda Ridge systems), ridge propagation and development of a continental margin rift (East Pacific Rise in the Gulf of California) (fig. 4–3), or more complex plate tectonic processes (Red Sea) can experience high rates of sedimentation by major rivers involving hemipelagic muds and (or) clastic sediments derived from adjacent continental crust. Today, about 5 percent of the world's active spreading centers are covered by sediment from nearby continental margins, including portions of the Juan de Fuca and Gorda Ridges in the northeast Pacific and the northern East Pacific Rise in the Gulf of California (Hannington and others, 2005). The high rates of sedimentation at these sites (10–100 cm/1,000 yr versus 1 cm/1,000 yr in the open ocean) result in thick sedimentary sequences that provide an effective density barrier to the eruption of relatively dense basalt on the seafloor. As a result, volcanic eruptions are rare at sedimented ridges, but subseafloor intrusions forming sill-sediment complexes are common (Einsele, 1985). Venting of high temperature hydrothermal fluids may occur around the margins of the buried sills, as in Middle Valley, the Escanaba Trough, and the Guaymas Basin today (Hannington and others, 2005). Although the sills may be partly responsible for driving hydrothermal circulation, high-temperature fluids mainly appear to originate in the volcanic basement where they are intercepted

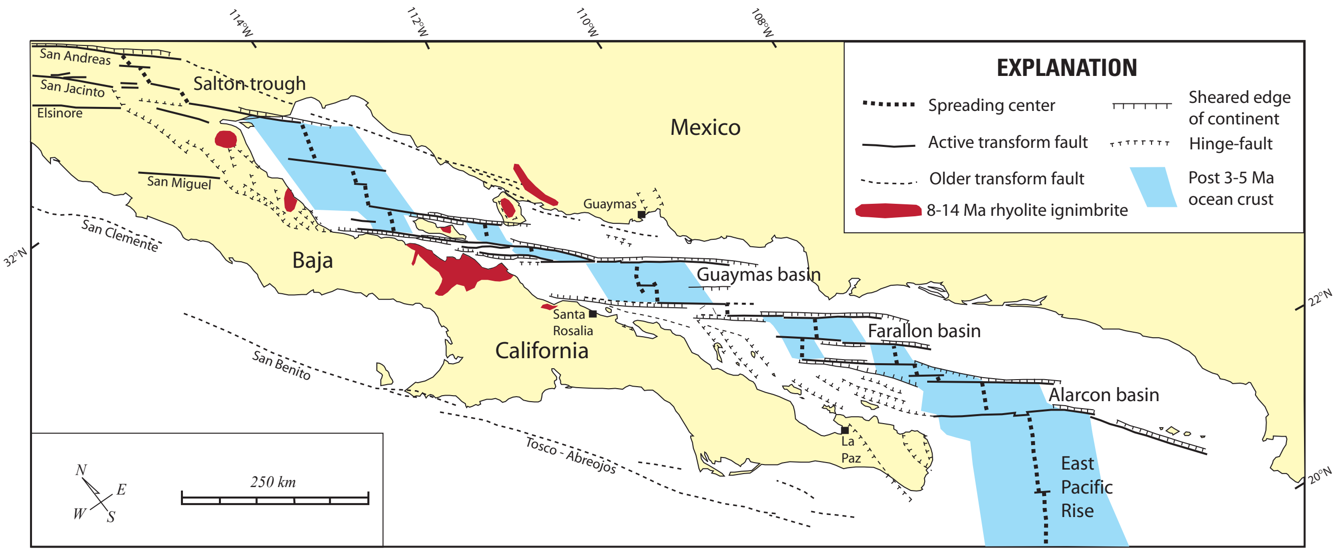

Figure 4–3. Structural map of the Gulf of California showing the extent of newly accreted oceanic crust in extensional basins (for example, Alarcon, Farallon, and Guaymas basins) along an extension of the East Pacific Rise. Massive sulfide mineralization is present in the Guaymas basin (Lonsdale and Becker, 1985). Modified from Lonsdale (1989).

along their flow path by basement highs and focused upward along growth faults or buried intrusions. At these sites, metals may be mainly deposited below the seafloor by replacement of the host sediment, resulting in sulfide deposits that are typically larger than deposits formed on bare mid-ocean ridges (Hannington and others, 2005) Also, because the high-temperature fluids may interact with continentally-derived clastic sediments as well as ocean crust, the sulfide deposits formed at sediment-covered ridges typically have different proportions of base and precious metals, particularly higher Pb and Ag contents (Franklin and others, 2005; Hannington and others, 2005). In some cases where rifting has resulted from propagation of an oceanic spreading axis into continental crust or from upwelling of the asthenosphere (for example, Red Sea), peralkaline rhyolites and transitional or alkaline basalts may be present in addition to the subalkaline suite (Barrett and MacLean, 1999).

Examples of ancient VMS deposits that appear to have formed in a sediment-covered ridge setting include the Triassic Windy Craggy deposit, Canada (Peter and Scott, 1999); the late Paleozoic Besshi deposit, Japan (Slack, 1993); the Neoproterozoic Ducktown deposit, United States (Slack, 1993); and the Miocene Beatson deposit, United States (Crowe and others, 1992).

Intraoceanic Volcanic Arcs and Related Back-Arc Rifts (Bimodal-Mafic Lithologic Association)

Volcanic arcs are curved chains of volcanoes that are convex toward the adjacent oceanic basin and separated from it by a deep submarine trench. Intraoceanic arcs have oceanic crust on either side and may overlie older arc volcanics, remnants of oceanic crust, and intrusive mafic-ultramafic bodies. Early intraoceanic arc volcanism is typically tholeiitic low-titanium (Ti) island-arc basalt and boninite (high-magnesium [Mg] andesite) (Stern and Bloomer, 1992; Pearce and Peate, 1995), but the summit calderas of the largest volcanoes commonly contain more silicic low-K volcanic rocks, including relatively abundant rhyolite pumice and postcaldera dacite-rhyolite lava domes (Fiske and others, 2001; Smith and others, 2003; Graham and others, 2008). Recent studies of several intraoceanic arcs in the western Pacific show that the overall volcanism is bimodal, with 30–50 percent of arc construction being dacitic to rhyolitic (≥63 weight percent [wt%] SiO_2) (Graham and others, 2008). As the arcs evolve, volcanism tends to become more andesitic and calc-alkaline. The tholeiitic island-arc basalts are mostly high-aluminum (Al) (≥16.5 wt% Al_2O_3) and are the product of partial melting of the mantle caused by the addition of H_2O and other volatiles to the sub-arc mantle through dehydration of subducting sediments and hydrated oceanic crust. The basalts differ from MORB by having (1) higher and more variable H_2O contents, (2) enrichments of large ion lithophile elements such as Cs, Rb, K, Ba, Pb, and Sr (strontium), and (3) relative depletions in high field strength elements, particularly Nb (niobium) and Ta (tantalum) (Pearce and Peate, 1995). These compositional characteristics are broadly consistent with the selective transport of elements by aqueous fluids derived from subducting sediments and oceanic crust. The felsic volcanic rocks associated with these intraoceanic arc volcanoes are generally highly vesicular and glassy, indicating degassing at depth and rapid cooling after mainly pyroclastic eruption during caldera formation (Graham and others, 2008). In addition, wide-angle seismic studies of some arcs indicate midcrustal layers with distinctive P-wave velocities that are interpreted as felsic intrusions (Crawford and others, 2003; Kodaira and others, 2007). The large volumes of silicic rocks present in intraoceanic arcs as well as their compositional heterogeneity, even from the same center, suggest that the silicic magmas are the result of dehydration melting of underplated arc material (Smith and others, 2003; Tamura and others, 2009).

Intraoceanic back-arc basins (regions of extension at convergent plate margins where rifting and, in some cases, seafloor spreading develops in the overriding plate) typically develop during periods of oceanward migration and sinking of the subducting plate (that is, slab rollback) and may accompany or follow episodes of arc extension and rifting (Clift and others, 1994; Marsaglia, 1995). The early rift phase of back-arc basin formation is characterized by development of structural grabens separated along strike by chains of volcanoes and structural highs (Taylor and others, 1991). Volcanism is bimodal, with predominantly basalt lava flows and cones and minor dacite and rhyolite lava flows in submarine calderas. Large quantities of volcaniclastic sediment derived from adjacent arc volcanoes may be deposited in the developing back-arc grabens (Clift and others, 1994). As extension continues and back-arc basins mature, seafloor spreading may commence with development of a spreading center similar to a mid-ocean ridge. Volcanism along the back-arc basin spreading center is tholeiitic basalt similar to MORB but is typically characterized by enrichments in large ion lithophile elements (for example, Cs, Rb, Ba, Th) and relative depletions in high field strength elements, particularly Nb and Ta (Pearce and Stern, 2006). These compositional attributes are attributed to interaction between the mantle and a component derived from the subducting slab of the arc system. The subduction signature of the back-arc basin basalts (BABB) tends to be greatest early in the evolution of the basin, when the spreading center is in closest proximity to the arc, and tends to diminish as the basin grows (Hawkins, 1995). High-temperature hydrothermal vents are commonly associated with back-arc volcanoes and spreading centers (Hannington and others, 2005).

The classic examples of modern intraoceanic arc–back-arc systems are the Izu-Bonin-Mariana arc and back-arc trough and the Lau Basin and Tonga-Kermadec arc and back-arc basin in the western Pacific (R.N. Taylor and others, 1992; Ewart and others, 1998). In both arc systems, early arc volcanism consists of low-K basaltic pillow lavas, hyaloclastite, and interbedded calcareous sediments. These rocks are overlain by strata cones consisting of basalt to andesite lavas and volcaniclastic deposits (Smith and others, 2003). Some larger volcanoes have experienced explosive caldera-forming eruptions involving dacitic to rhyolitic pyroclastics that occurred at depths of at least 1,500 m (see Fiske and others, 2001; Smith and others, 2003). High-temperature hydrothermal venting is present in many of the calderas (de Ronde and others, 2003) and is typically localized along caldera walls or on postcaldera felsic domes (Fiske and others, 2001; Wright and others, 2002). The venting generally occurs at shallower water depths than that on mid-ocean ridges or back-arc spreading centers (Hannington and others, 2005), resulting in widespread boiling and hydrothermal fluids venting at generally lower temperatures. In addition, the presence of sulfur-rich fumaroles and low-pH vent fluids provides evidence of the direct input of magmatic volatiles to the hydrothermal fluids. At least some of these intraoceanic arc hydrothermal systems appear to be transitional to magmatic-hydrothermal systems in subaerial arc volcanoes and are characterized by distinctive polymetallic sulfides and Au-Ag-barite-rich deposits (Hannington and others, 1999).

High-temperature hydrothermal vents are present in the back-arc basins associated with both the Izu-Bonin-Mariana and Tonga-Kermadec arc systems. In the Mariana Trough, high-temperature hydrothermal activity occurs both at an axial volcano along the back-arc spreading center and at a number of back-arc volcanoes immediately behind the arc front (Ishibashi and Urabe, 1995; Stuben and others, 1995). In the Lau Basin behind the Tonga arc, black smoker activity resembling typical mid-ocean ridge hydrothermal vents occurs on the northern Lau spreading center and is hosted by typical MORB basalt. In contrast, vent activity in the south Lau Basin is hosted mainly by arclike andesite and deposits contain abundant barite, as well as much higher Pb, As, Sb, Ag, and Au (Hannington and others, 1999). The north to south change in the nature of back-arc magmatism and black smoker activity in the Lau Basin corresponds with (1) a significant change in width of the basin from about 600 km in the north to only about 200 km in the south, (2) a decrease in the spreading rate from about 10 cm/yr in the north to about 4 cm/yr in the south, (3) a decrease in axial water depth from 2,300–2,400 m in the north to about 1,700 m in the south, and (4) a decrease in the distance of the back-arc spreading center to the active arc, which approaches to within about 20 km of the arc in the southern part of the basin (Hannington and others, 2005).

Although high-temperature hydrothermal vents and massive sulfide deposits are present in some volcanoes at the front of intraoceanic arcs, these deposits are expected to be relatively small because of smaller hydrothermal circulation cells related to small, shallow magma chambers beneath the summit calderas of the stratovolcanoes (Hannington and others, 2005). The presence of abundant pyroclastic deposits formed during explosive eruption events in these submarine arc volcanoes (Fiske and others, 1998, 2001) also suggests that the hydrothermal systems would experience frequent disruptions. In addition, shallow water depths and lower confining pressures at the summits of these arc volcanoes can result in subseafloor boiling and development of vertically extensive stockwork mineralization rather than development of large seafloor massive sulfide deposits. From recent studies of intraoceanic volcanic arcs and related back-arc rift systems, as well as from comparisons with the geologic record, it appears that the potential for the formation of large massive sulfide deposits is greatest behind the arc (that is, associated with arc rifting and back-arc development) rather than at the volcanic front (Hannington and others, 2005).

Ancient examples of VMS deposits that are interpreted to have formed in intraoceanic volcanic arc–back-arc settings include the Archean Kidd Creek deposit, Canada (Barrie and others, 1999); the Paleoproterozoic Crandon deposit, United States (DeMatties, 1994); the Ordovician Bald Mountain deposit, United States (Schulz and Ayuso, 2003); the Permo-Triassic Kutcho Creek deposit, Canada (Barrett and others, 1996); and the Jurassic-Cretaceous Canatuan deposit, Philippines (Barrett and MacLean, 1999).

Continental Margin Arcs and Related Back-Arc Rifts (Bimodal-Felsic and Felsic-Siliciclastic Lithologic Associations)

Submarine magmatic arcs and related back-arc basins that develop in a basement of extended continental crust, pre-existing arc crust, or entirely in a basement of continental crust (continental margin arc–back-arc system) are characterized by increased amounts of felsic volcanic rocks and more complex chemistry of both arc and back-arc magmas, which can range from MORB-like basalt compositions to medium and high-K calc-alkaline and shoshonitic andesite, dacite, and rhyolite (Barrett and MacLean, 1999). In addition, there can be considerable overlap of magma sources, which can result in arclike magmas being erupted in the back-arc region. Particularly in continental margin arcs and back-arcs, the abundance of felsic volcanic rocks may reflect both greater extents of fractional crystallization of magmas trapped in thickened crust and direct partial melting of continental crust. Because of their proximity to continental crust, continental margin arc–back-arc systems also can receive large amounts of siliceous clastic sediment.

The modern Okinawa Trough and Ryukyu arc south of Japan are examples of a continental back-arc rift and margin arc, respectively. In this region, oblique northward subduction of the Philippine Sea plate has led to development of a back-arc basin that varies in width from about 230 km in the north to only 60–100 km in the south. In the north, the basin is characterized by diffuse extensional faulting and water depths of only a few hundred meters. In contrast, the central part of the Okinawa Trough consists of several en echelon grabens 50–100 km long and 10–20 km wide at water depths up to 2,300 m. The variation in depth and style of rifting corresponds with major differences in crustal thickness, which ranges from 30 km in the north to only 10 km in the south (Sibuet and others, 1995). Also varying from north to south is the thickness of sedimentary cover, which is up to 8 km in the north but only about 2 km in the south. The individual grabens in the central Okinawa Trough contain a number of volcanic ridges or elongate volcanoes composed of a bimodal calc-alkaline suite of vesicular basalt, andesite, and rhyolite (Shinjo and Kato, 2000). Hydrothermal activity is widespread around the volcanic ridges, but the largest vent field (JADE) is located in a structural depression (Izena cauldron) floored by basalt and andesite with local dacite and rhyolite lava domes and a cover of rhyolite pumice and mudstone (Halbach and others, 1989). Polymetallic sulfides in the JADE field are distinctly rich in Pb, As, Sb, Hg, Ag, Au, and Ba (Halbach and others, 1993).

Ancient examples of VMS deposits that are interpreted to have formed in continental margin arc–back-arc settings include the Miocene Kuroko deposits in Japan (Ohmoto and Skinner, 1983); the Ordovician Brunswick No. 12 and other deposits in the Bathurst mining camp, Canada (Goodfellow and McCutcheon, 2003); the Jurassic Eskay Creek deposit, Canada (Barrett and Sherlock, 1996); and deposits in the Devonian-Mississippian Bonnifield district, United States (Dusel-Bacon and others, 2004).

Temporal (Secular) Relations

Volcanogenic massive sulfide deposits have formed in extensional submarine volcanic settings that range in age from Paleoarchean (3.55 Ga) to Recent, with deposits actively forming today at mid-ocean ridges and oceanic volcanic arcs and back-arc basins. However, deposits are not uniformly distributed through time but are concentrated particularly in late Archean (2.85–2.60 Ga), Paleoproterozoic (2.0–1.7 Ga), Neoproterozoic (900–700 mega-annum [Ma]), Cambro-Ordovician (550–450 Ma), Devono-Mississippian (400–320 Ma), and Early Jurassic to Recent (200–0 Ma) subaqueous volcanic sequences (fig. 4–4*A*; see also Galley and others, 2007). Similarly, the total tonnage and contained metal content of VMS deposits are concentrated in late Archean (2.85–2.60 Ga), Paleoproterozoic (2.0–1.7 Ga), lower Paleozoic (550–450 Ma), upper Paleozoic (400–320 Ma), and Early Jurassic to Recent (200–0 Ma) sequences (fig. 4–4*H*). Deposits less than 15 Ma (middle Miocene) are almost all associated with modern ocean settings (Franklin and others, 2005; Mosier and others, 2009), due to limited obduction of younger marine volcanosedimentary sequences onto the continents. The heterogeneous temporal distribution of VMS deposits can be ascribed to the balance between a deposit's formation under specific conditions in particular geodynamic settings and its preservation once formed (Groves and Bierlein, 2007). Most VMS deposits preserved in the geologic record formed in subduction-related oceanic and continental volcanic arc and back-arc settings, and their temporal distribution corresponds closely with periods of major ocean-closing and terrane accretion following the breakup of large continents (Barley and Groves, 1992; Titley, 1993; Groves and others, 2005). However, it is likely that most VMS deposits have been lost from the geologic record either by oxidation at the seafloor or through accretion, uplift, and erosion in marginal orogenic belts during supercontinent assembly (Barley and Groves, 1992; Groves and others, 2005).

The different VMS deposit types also show temporal variations in abundance (figs. 4–4*C-G*). Deposits in the bimodal-mafic association are most common in the Archean and Paleoproterozoic, but they are also important constituents in the Mesozoic and Cenozoic. In contrast, deposits in the mafic-ultramafic association are almost all Paleozoic and younger, except for a small group of Paleoproterozoic deposits (fig. 4–4*G*), reflecting the subduction of most ancient ocean floor along convergent margins. The siliciclastic-mafic and felsic-siliciclastic deposits are mainly Mesozoic, while bimodal-felsic deposits are more evenly distributed although less common in the Precambrian. These variations in deposit types over time also reflect fundamental changes in tectonic style through time, as well as differences in preservation of different tectonic settings (Franklin and others, 2005; Groves and others, 2005). The relatively rare occurrence in the early Precambrian of both siliciclastic-mafic and felsic-siliciclastic deposit types suggests that extensional continent margin tectonic settings were less common during the early evolution of the Earth.

Duration of Magmatic-Hydrothermal System and Mineralizing Processes

Volcanogenic massive sulfide deposits are the product of volcanically generated hydrothermal systems developed at a specific time interval or intervals in the evolution of submarine volcanic sequences. Structural, lithostratigraphic, and geochemical characteristics of these submarine volcanic sequences indicate that they formed during periods of extension. In most arc-related settings, peak extension or rifting is short lived and often marked by the occurrence of high silica volcanic rocks (dacite to rhyolite) and their intrusive equivalents. It is during these short lived periods of extension, typically lasting less than 2 to 3 m.y., that VMS deposits are formed (Franklin and others, 2005).

Two major factors help control the fluid flow, discharge duration, and life span of a VMS-forming hydrothermal system (Schardt and Large, 2009): (1) the nature, depth, and size of the heat source, and (2) the temporal permeability distribution in the rock units and faults. The results of recent numerical computer simulations of ancient and modern VMS systems (see review in Schardt and Large, 2009) suggest that the duration of significant hydrothermal fluid discharge ($T>150$ °C) can last anywhere from 400 years to >200,000 years. These results are comparable to average radiometric dates determined for modern seafloor hydrothermal systems (<1,000 to about 250,000 years; Lalou and others, 1995; Scott, 1997). Numerical computer simulations conducted by Schardt and Large (2009) suggest that in a hydrothermal fluid with seawater salinity, 10 parts per million (ppm) Zn+Cu, and a

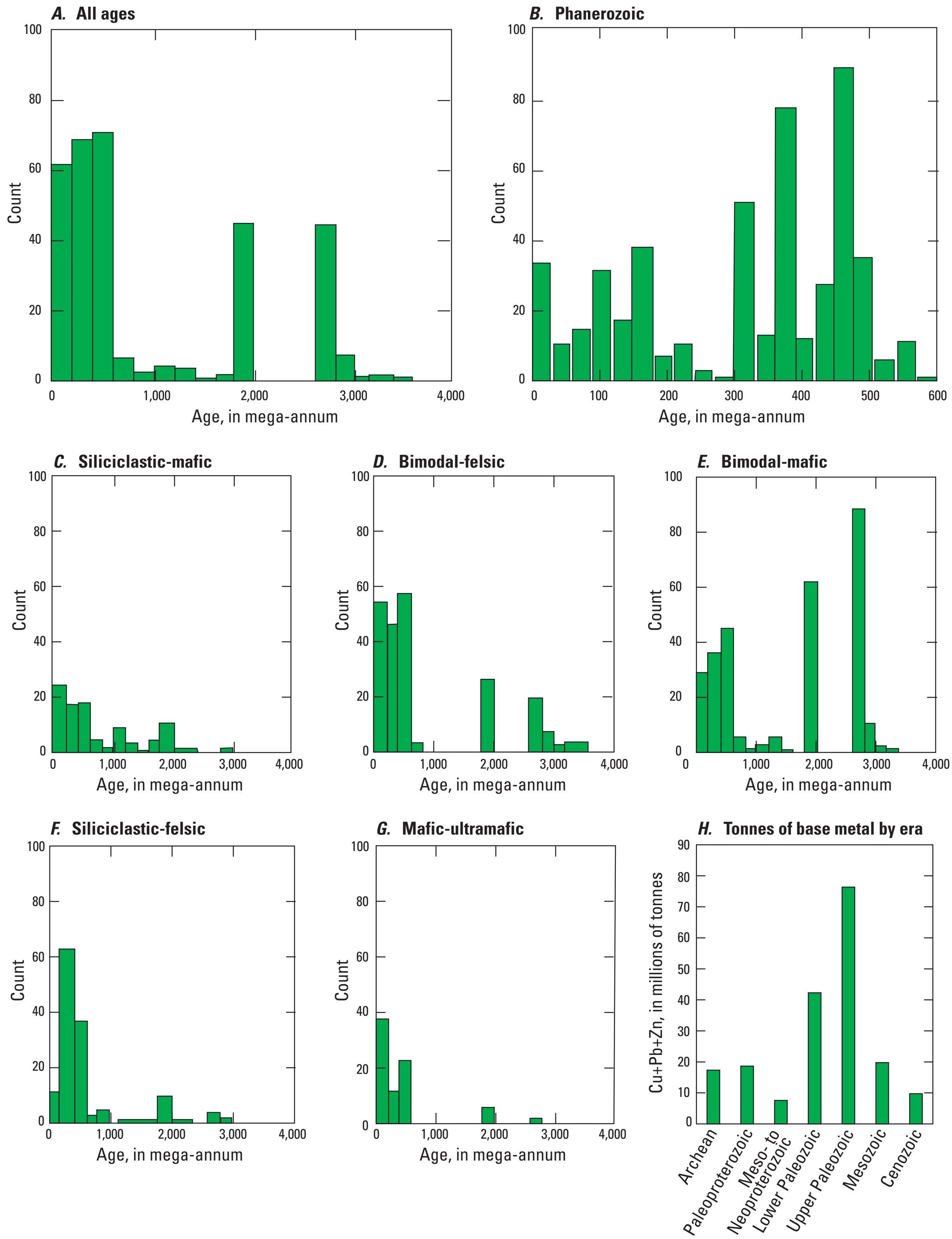

Figure 4–4. Histograms showing (*A–G*) number of volcanogenic massive sulfide deposits and (*H*) tonnage of contained metal of Cu + Zn + Pb in million tonnes versus age in million years. Data revised from Mosier and others, 2009. [Cu, copper; Pb, lead; Zn, zinc]

deposition efficiency greater than 10 percent, an average VMS deposit (1.2 Mt total metal) could form within a time frame of less than 5,000 years to as long as 14,000 years, depending on geologic conditions such as temperature and depth of the heat source. Fluids carrying lower amounts of metals are unlikely to deposit sufficient base metals to form an average size deposit, whereas a lower deposition efficiency (<10 percent) would require a much longer time to form such a deposit. Formation of a giant (>1.7 Mt Zn or 2 Mt Cu total metal) and supergiant deposit (>12 Mt Zn or 24 Mt Cu total metal) requires (a) a fluid with a higher metal content in solution (>10 ppm), (b) a deposition efficiency exceeding 10 percent, and (or) (c) a longer time to accumulate sufficient metals. Higher salinity hydrothermal fluids have increased metal-carrying capacity and would improve chances of forming a large base metal deposit.

Studies of the TAG hydrothermal field, located on the slow-spreading Mid-Atlantic Ridge at 26°N, have shown that activity began about 100,000 to 150,000 years ago with low-temperature fluids forming stratiform Mn-oxide deposits (Lalou and others, 1995). High-temperature hydrothermal events, which first started about 100,000 years ago in the Mir zone within the TAG field, have been episodic and generally followed periods of basalt extrusion at an adjacent pillow lava dome. The correlation between the hydrothermal and volcanic events supports the interpretation that episodic intrusions at the volcanic center supplied the heat to drive episodic hydrothermal activity at the adjacent TAG sulfide mound (Rona and others, 1993). The radiometric studies at the TAG field show that hydrothermal venting may be reactivated in the same area and that periods of activity and quiescence may alternate with a periodicity of thousands of years (Lalou and others, 1995).

Relations to Structures

Many VMS deposits occur in clusters or districts about 40 km in diameter that contain about a dozen relatively evenly spaced deposits, one or more of which contains more than half of the district's resources (Sangster, 1980). Controls on the localization of VMS deposits mainly involve volcanic and synvolcanic features. Such features include, but are not limited to, calderas, craters, grabens, and domes; faults and fault intersections; and seafloor depressions or local basins. Identification of these types of controls is generally limited to relatively undeformed deposits with minimal or no postore structural overprint.

In most cases, localization of sulfide mineralization involved structural preparation of a plumbing system including the development of permeable conduits for metalliferous hydrothermal fluids. Faults show the most fracturing around fault tip-lines (breakdown regions), the curvilinear trace of the fault termination, where stresses associated with the displacement gradient are concentrated and drive crack propagation into non-fractured rock (Curewitz and Karson, 1997). Where two or more fault tip-lines are in close proximity, the individual breakdown regions merge, forming a single, modified breakdown region. Curewitz and Karson (1997) have shown that the structural setting of hydrothermal vents varies based on the geometry of the fault system and the mechanisms that create and maintain permeable pathways for fluid flow (fig. 4–5). Their global survey of hydrothermal vents showed that 78 percent are near faults and 66 percent of the vents at mid-ocean ridges are in fault interaction areas (Curewitz and Karson, 1997). Detailed studies along both fast-spreading mid-ocean ridges (for example, Haymon and others, 1991) and slow-spreading ridges (for example, Kleinrock and Humphris, 1996) confirm the prevalence of hydrothermal venting in areas of fault interaction. In addition, recent studies near slow- and ultraslow-spreading segments of the Mid-Atlantic Ridge have shown that high-temperature black smoker fluids have been focused above low-angle detachment faults (fig. 4–6; McCaig and others, 2007). Intense metasomatic and isotopic alteration in the fault rocks along these detachment structures show that large volumes of fluid have been focused along them resulting in potentially long-lived hydrothermal systems and large massive sulfide deposits (Lalou and others, 1995; McCaig and others, 2007).

The preferential alignment of ancient VMS deposits and their proximity to volcanic vent areas and synvolcanic faults demonstrates a pronounced structural control on their location (for example, Hokuroku district; Scott, 1980). The orientation of synvolcanic faults in extensional environments is controlled by the direction of least principal stress during periods of extension and volcanism (Cox and others, 2001). The principal extensional direction can be subhorizontal and perpendicular to the rift axis or, in more complex cases such as transtensional rifts, oriented oblique to the rift axis (Kleinrock and others, 1997). The synvolcanic faults provide loci for magma migration as well as for hydrothermal fluid discharge. Features useful in identifying synvolcanic faults in ancient volcanic sequences (Franklin and others, 2005) include: (1) local discontinuities in the stratigraphy of footwall sections; (2) diachronous wedges of talus; (3) debris flows that thicken or terminate over a short lateral distance; (4) transgressive alteration zones; (5) synvolcanic dikes and dike swarms, particularly those that terminate in either cryptodomes or at intravolcanic sedimentary horizons; (6) the location of felsic lava flows, domes, and cryptodomes marking a volcanic center; and (7) the preferential alignment of volcanic vents.

Volcanic collapse structures in submarine settings are mainly calderas, craters, and grabens. For example, recent studies along the Izu-Bonin arc–back-arc system in the western Pacific Ocean have discovered several moderate- to deep-water calderas characterized by rhyolite pumice (Fiske and others, 1998, 2001; Yuasa and Kano, 2003) and hydrothermal massive sulfide mineralization (Ishibashi and Urabe, 1995; Iizasa and others, 1999). Studies have interpreted submarine calderas to be settings for several ancient VMS deposits and districts, based on comparisons with the settings of modern seafloor hydrothermal systems. (see Ohmoto, 1978; Stix and others, 2003; Mueller and others, 2009). Ancient VMS

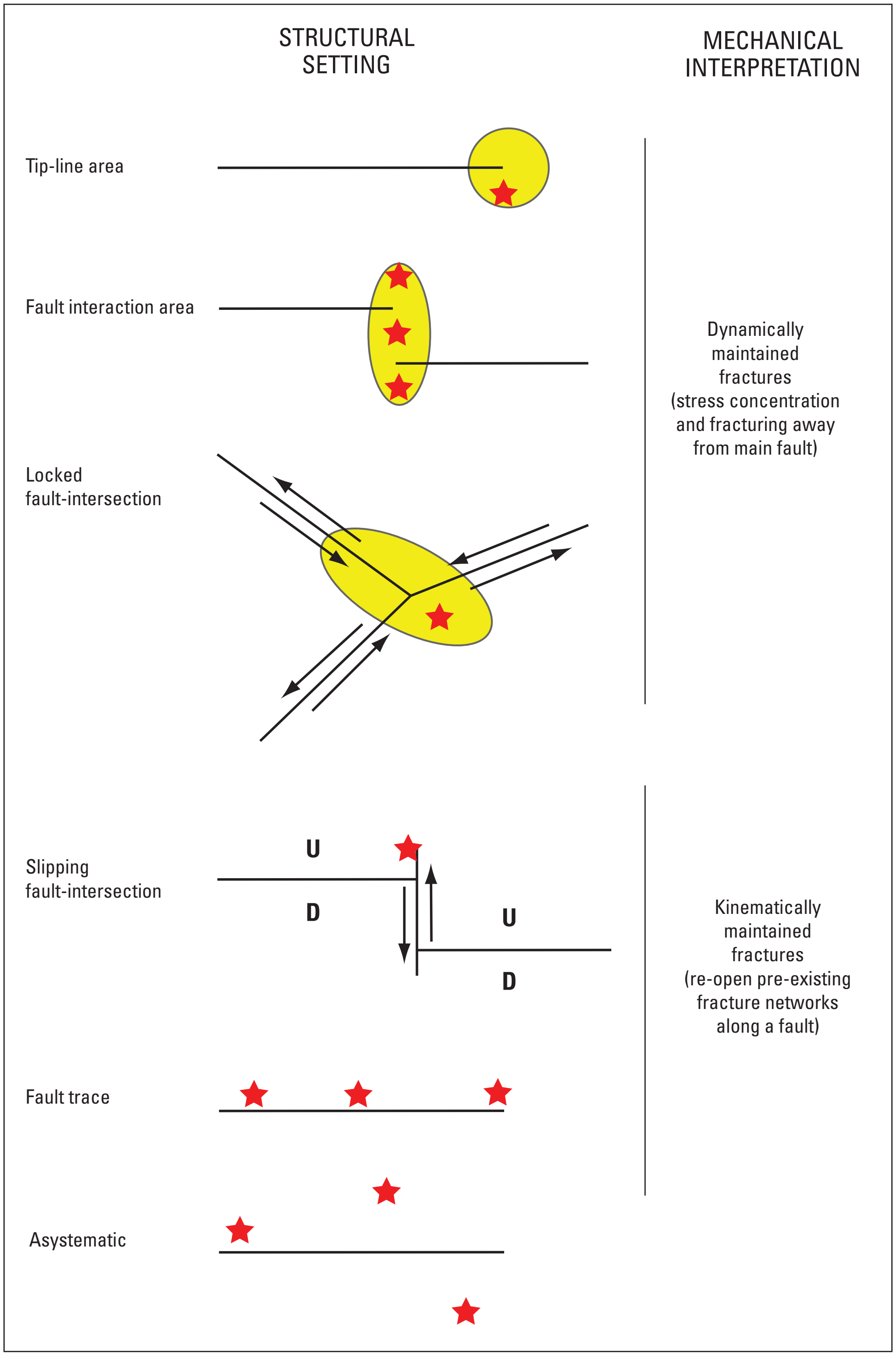

Figure 4–5. Schematic diagram showing examples of the different structural settings of hydrothermal vents (red stars) relative to faults (straight lines) and breakdown regions (yellow shaded areas). In the upper three examples, vents are located in areas of stress concentration and are fracturing away from the main fault (dynamically maintained fractures), while in the next three examples the vents are located along the fault in re-opened, pre-existing fracture networks (kinematically maintained fractures). After Curewitz and Karson (1997).

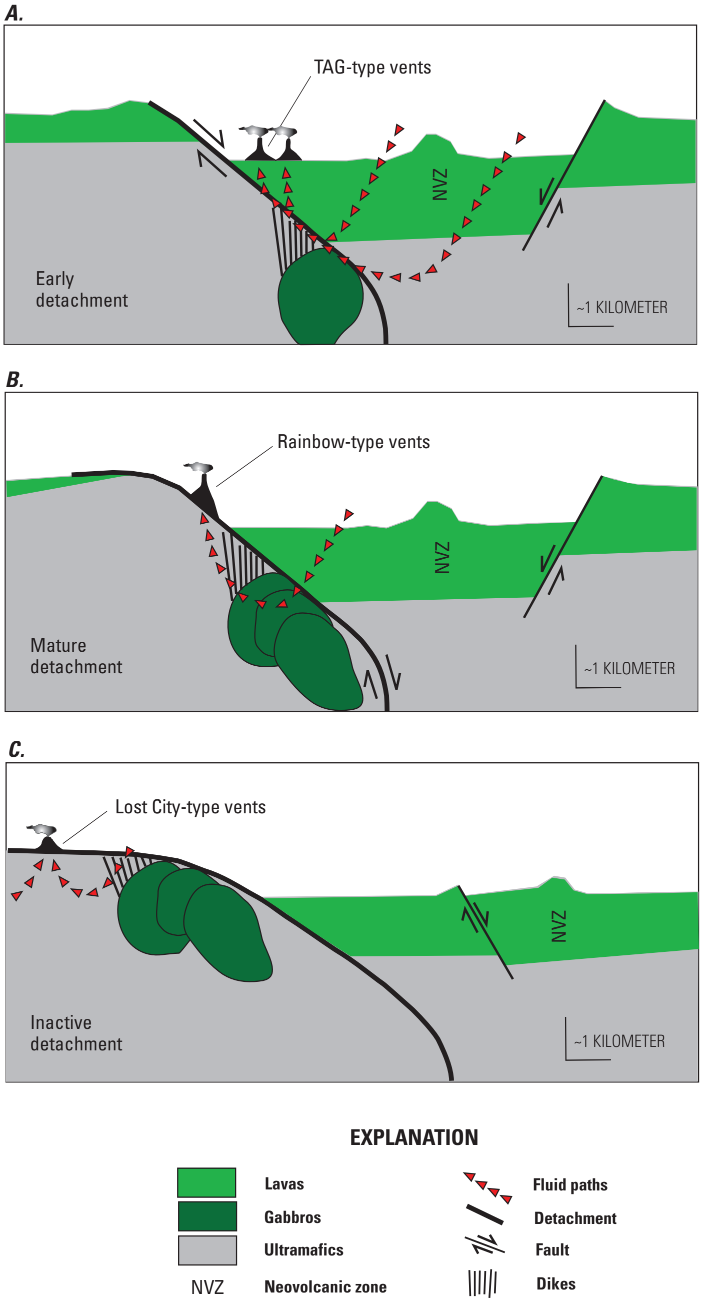

Figure 4–6. Model for fluid circulation and types of hydrothermal venting related to the development of detachment faults along slow-spreading mid-ocean ridges. Modified from McCaig and others (2007). [TAG, Trans-Atlantic Geothermal]

deposits that have interpreted caldera structure settings include those of the Hokuroku district in Japan (Scott, 1980; Ohmoto and Takahashi, 1983), the Sturgeon Lake district in Ontario (Morton and others, 1991; Hudak and others, 2003; Mumin and others, 2007), and the Hunter Mine Group in the Noranda district in Quebec (Mueller and Mortensen, 2002; Mueller and others, 2009). Possible structural controls within such caldera settings include ring faults and their intersections with regional arc or back-arc faults, hinge faults along asymmetric trapdoor-type collapse structures, and volcanic domes and their margins. A volcanic-related graben was evoked by Slack and others (2003) and Busby and others (2003) as having controlled the location and geometry of the thick, bowl-shaped Bald Mountain deposit in Maine. In the Noranda district of Quebec, some massive sulfide orebodies such as Millenbach are localized within former volcanic vents on a series of structurally-aligned rhyolite domes (Knuckey and others, 1982; Gibson and Galley, 2007). A detailed structural analysis by Mumin and others (2007) of VMS deposits within the south Sturgeon Lake caldera, Ontario, showed that massive sulfides occur preferentially along faults and fissures related to the formation of synvolcanic rifts and grabens. The types and styles of favorable structures reflect: (1) the composition, competency, and alteration of the host rocks; (2) the history of synvolcanic tectonism including extension-related collapse; and (3) orthogonal faulting and shearing. In the Golden Grove deposit, Western Australia, a synvolcanic growth fault is inferred by Sharpe and Gemmell (2002) to coincide with the highest grades of Cu (±Au) and the thickest zones of massive sulfide, magnetite, and footwall feeder zone mineralization.

The spatial-temporal conditions that control the formation of submarine calderas also may largely determine the size and location of contained VMS deposits (Stix and others, 2003). Field studies and experimental work show that two main types of faults develop during caldera collapse: (1) inner faults, which generally dip outward and accommodate the majority of displacement, and (2) outer, inward-dipping faults associated with late-stage peripheral extension, normal faulting, and down sagging as the caldera collapses (Stix and others, 2003; Kennedy and others, 2004). In areas of extension and transtension, the main caldera faults may not be circular, but instead may be significantly more asymmetric (Kennedy and others, 2004). When these linear and arcuate structures intersect, the resulting fracture system is better developed than in other areas of the caldera and therefore forms particularly favorable sites for hydrothermal circulation and the formation of mineral deposits. In addition, asymmetric calderas formed by subsidence either as a trapdoor along a single hinge fault or as a series of blocks (Heiken and others, 1986; Wohletz and Heiken, 1992) appear to provide structural settings that are particularly favorable for the formation of certain VMS deposits (Mueller and others, 2009). The formation of VMS deposits appears favored

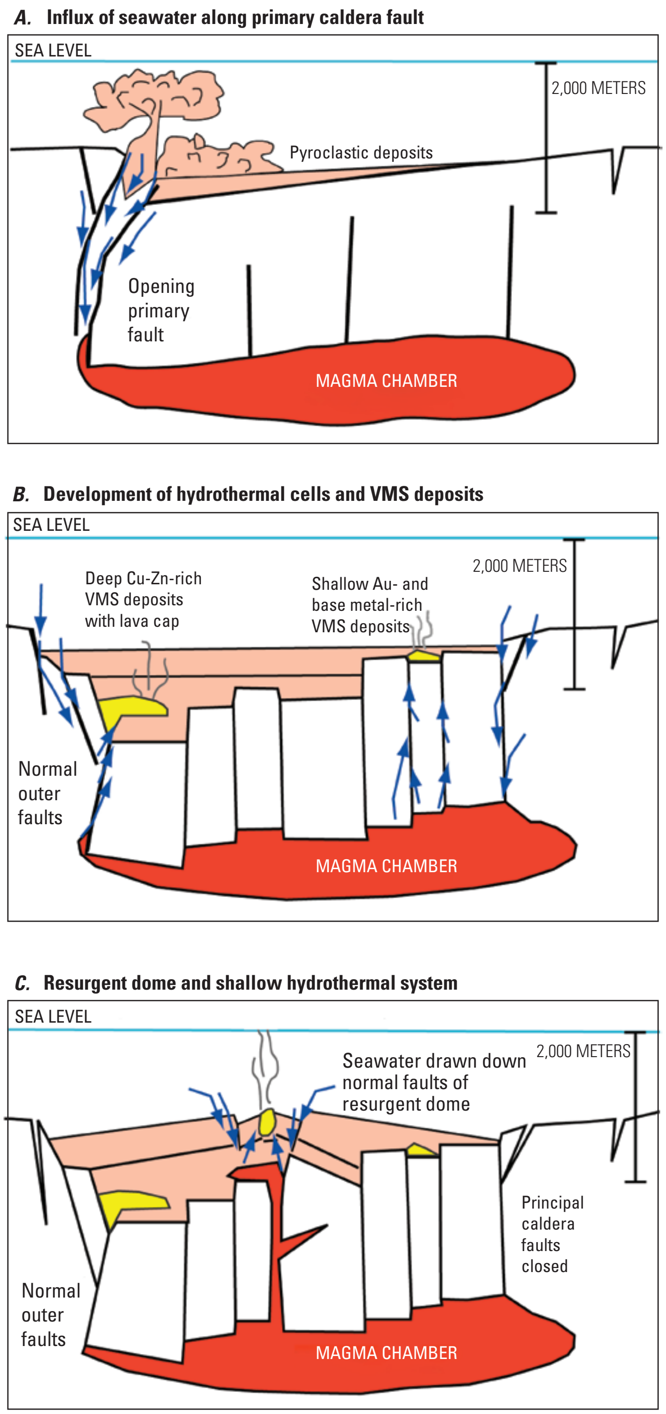

Figure 4–7. (left) Conceptual diagram showing the evolution of a caldera-related submarine magmatic-hydrothermal system. *A*, Asymmetric collapse of the caldera allows influx of seawater along opening caldera margin fault; erupted pyroclastic deposits pond within the developing asymmetric basin. *B*, Cold seawater flows downward along outer inward-dipping faults, while hot mineralizing fluids move up along a series of outward-dipping faults resulting from piecemeal caldera collapse. As a result, massive sulfide deposits can form in a number of locations and possible water depths within the caldera. *C*, Caldera resurgence, related to renewed magmatism and intrusion into roof rocks above the main magma chamber, is accompanied by the formation of tensional faults as the center of the caldera is uplifted. This permits additional hydrothermal fluid circulation and formation of additional massive sulfide deposits in the central parts of the caldera. Modified from Stix and others (2003). [VMS, volcanogenic massive sulfide; Au, gold; Cu, copper; Zn, zinc]

at two stages of caldera formation (fig. 4–7): (1) during and immediately after caldera collapse and (2) during post-caldera resurgence accompanying re-injections of magma at shallow depth. During the initial subsidence of an asymmetric caldera, a magmatic-hydrothermal system is opened and exposed along the main outward-dipping caldera faults (fig. 4–7*A*). This opening promotes greater magma degassing and provides opportunity for large influxes of seawater or local meteoric water that may interact directly with the magma reservoir. Over time, the initially deep hydrothermal system migrates upward along inner caldera faults, while simultaneously the hydrothermal system is recharged through the peripheral faults (fig. 4–7*B*). Metals may be supplied to the hydrothermal fluid directly by magma degassing and by high-temperature leaching from the volcanic rocks. The largest VMS deposits are generally developed in porous pyroclastic deposits adjacent to caldera-bounding faults (Stix and others, 2003; Mueller and others, 2009). During post-caldera resurgence, the injection of new magma can cause uplift of the caldera floor and reactivation of the hydrothermal system as open fluid pathways develop along tensional faults (fig. 4–7*C*).

Summit calderas on submarine arc-front volcanoes are generally relatively small (<10 km across) and are expected to have only small hydrothermal systems and correspondingly small but potentially high grade massive sulfide deposits (Hannington and others, 2005). However, recent surveys in the western Pacific have shown that such calderas and associated hydrothermal activity are much more common than previously recognized (de Ronde and others, 2007). In addition, calderas are rarely simple constructions because, over time, they can evolve into composite structures, including nested or overlapping caldera complexes (Mueller and others, 2009). In the geologic record, such complex calderas can host major massive sulfide resources (Mueller and others, 2009; Pearson and Daigneault, 2009). In general, calderas on intraoceanic arc volcanoes are smaller than those developed on continental-margin arc volcanoes (Smith, 1979).

Structural controls also have been proposed for VMS deposits that lack definitive evidence of a caldera setting. For example, in back-arc areas where the crust is actively rifting, large seafloor depressions or cauldrons may develop, such as the DESMOS cauldron in the eastern Manus Basin and the Izena cauldron in the Okinawa Trough (Hannington and others, 2005). The DESMOS cauldron in the eastern Manus Basin north of New Britain is located in extended crust between ridges of vesicular calc-alkaline basalt to rhyolite volcanic rocks. Hydrothermal venting occurs along a 10-km strike length, and drilling has recovered sulfide-impregnated volcaniclastic rocks from the top of a ridge to 380 m below the seafloor. In the central part of the Okinawa Trough, back-arc volcanism and hydrothermal activity occurs within several en echelon grabens. The individual grabens are 50–100 km long, 10–20 km wide, and contain a number of volcanic ridges or elongate volcanoes comprising bimodal vesicular calc-alkaline basalt, andesite, and rhyolite. Hydrothermal activity occurs on or adjacent to the volcanic ridges with the largest vent field (JADE) located in a 5×6-km-wide and 300-m-deep structural depression known as the Izena cauldron. Other examples include the Tambo Grande deposit in Peru, attributed by Tegart and others (2000) to localization in structurally-bound troughs and second-order grabens, and the San Nicolás deposit in Mexico, where syndepositional faults and the steep flank of a rhyolite dome appear to have focused massive sulfide mineralization, according to Johnson and others (2000).

One indirect structural control for VMS deposits is their proximity to large subvolcanic sills, occurring as much as 2,000 m in the footwall of some deposits, which not only provide significant heat to drive hydrothermal systems, but also can increase fracturing of host volcanic strata and focus hydrothermal fluids towards the seafloor (see Galley, 2003; Carr and Cathless, 2008). Heat flow data for modern submarine systems in Guaymas Basin, Gulf of California, further suggest that the hydrothermal fluids are localized in fractures within the sills and along their margins (Lonsdale and Becker, 1985). Finite element modeling to simulate the deposit size and spatial distribution of VMS deposits above the Bell River Complex in the Matagami District in Quebec (Carr and Cathless, 2008) shows that a simple dependence of host rock permeability on temperature localizes hydrothermal upwelling above the intrusive complex and produces a spatial pattern and range of vented fluid volumes similar to that found in the Matagami District. Similarly, three-dimensional modeling of the structure and dynamics of mid-ocean ridge hydrothermal systems has demonstrated that convection cells self-organize into pipelike upflow zones spaced at regular distances of roughly 500 m surrounded by narrow zones of focused and relatively warm downflow (Coumou, and others, 2008). These results closely approximate the regularly spaced high-temperature vents of the Main Endeavour Field on the Juan de Fuca Ridge (Tivey and Johnson, 2002).

Other depositional controls relate mainly to paleotopography. Seafloor depressions, regardless of origin, serve as local basins for the deposition of both chemically and mechanically deposited sulfides. Chemically-precipitated sulfides preferentially accumulate in topographically low areas, especially in cases where the vent fluids are high-salinity brines that are denser than ambient seawater, forming local metalliferous brine pools (see Large, 1992; Solomon, 2008). Seafloor depressions also localize clastic sulfides eroded from sulfide-rich chimneys, mounds, and other edifices. In many deposits, these sulfides consist of sand- to silt-sized polymictic grains that preserve graded bedding and other sedimentary features. Rarely, VMS-derived debris flows contain cobble- to boulder-size clasts of massive sulfide that accumulated in elongate channels that extend as much as 1 km or more along strike from their in situ source, such as in the high-grade, transported orebodies at Buchans, Newfoundland, Canada (Walker and Barbour, 1981; Binney, 1987).

Relations to Igneous Rocks

Volcanogenic massive sulfide deposits form at or near the seafloor in extensional geodynamic settings in spatial, temporal, and genetic association with contemporaneous volcanism. The deposits are often directly hosted by, or occur in, volcanic-dominated sequences, but they also can occur in sediment-dominated sequences in association with periods of volcanic-intrusive activity. In mafic-dominated juvenile environments (for example, mafic-ultramafic, bimodal-mafic, and siliciclastic-mafic lithologic associations), VMS deposits are associated with boninite and low-Ti island-arc tholeiite, mid-ocean ridge basalt (MORB), or back-arc basin basalt (BABB) (Barrett and MacLean, 1999). Felsic rocks in mafic-dominated juvenile settings are typically tholeiitic and relatively depleted in trace elements (Barrett and MacLean, 1999; Hart and others, 2004). In environments associated with continental crust and typically dominated by felsic magmatism (for example, bimodal-felsic and felsic-siliciclastic lithologic associations), VMS-associated mafic rocks can include tholeiitic, calc-alkaline, and alkaline basalts and andesites, with the felsic rocks typically ranging from calc-alkaline dacite-rhyolite to trace element enriched peralkaline compositions (Lentz, 1998; Barrett and MacLean, 1999; Hart and others, 2004). The major relationships between volcanic activity and VMS deposits include: (1) controls on the localization of deposits in volcanic and synvolcanic structures and lithologic units (Gibson and others, 1999); (2) production of high rates of heat advection to the near surface environment that drives seawater convection and fluid-rock interaction in footwall rocks (Schardt and Large, 2009); and (3) contributions of metals and sulfur through reaction of footwall rocks with convecting fluid and (or) directly from magmatic-hydrothermal fluids (de Rhonde, 1995; Yang and Scott, 1996; Franklin and others, 2005; Yang and Scott, 2006).

Studies of modern hydrothermal activity on mid-ocean spreading centers of all spreading rates demonstrate that high-temperature vent fields are almost universally associated with the presence of magma; "hot rock" or nonmagmatic heat sources appear insufficient to generate high-temperature hydrothermal activity (Baker, 2009). In ancient volcanic sequences, composite synvolcanic intrusions are often present in the footwall below VMS deposits and are taken to represent the heat engine that initiated and sustained the subseafloor hydrothermal activity that formed the deposits (Galley, 2003, and references therein). At ocean spreading-ridge settings magma may rise to within a few thousand meters of the seafloor and form elongate gabbroic sills that parallel the seafloor-spreading axis (Stinton and Detrick, 1992; Perk and others, 2007). In settings with pre-existing ocean floor and arc crust, mafic magmas may underplate the crust and produce intermediate to felsic partial melts that form bimodal intrusive/extrusive assemblages (Lentz, 1998). The resulting composite (gabbro-diorite-tonalite-throndhjemite) intrusive complexes may rise to within 2–3 km of the seafloor, while underplating and extension in thicker (20–30 km) crust may result in mid-crustal intrusions (Galley, 2003). Gibson and others (1999) note that, in ancient VMS-hosting sequences, synvolcanic intrusions can be recognized by: (1) their sill-like, composite nature; (2) weak or absent contact metamorphic aureole; (3) similar composition to rocks of the host volcanic sequence; (4) similar, but commonly younger, age; (5) the presence of hydrothermal alteration assemblages similar to those in the host volcanic rocks; and (6) the presence of base metal (Cu, Mo) and (or) gold mineralization.

Volcanogenic massive sulfide deposits bear a close relation to the volcanic lithofacies association that hosts them (Gibson and others, 1999); the rocks of the footwall (and immediate hanging wall) record the environment in which the deposits form and the environment that influenced the deposit morphology, mechanisms of sulfide accumulation and composition, and geometry and mineralogy of alteration assemblages (Gibson and others, 1999; Franklin and others, 2005). In addition, hanging-wall strata provide a record of the duration and termination of the mineralization event and indicate how the deposit was preserved. Three end member lithofacies subdivisions have been defined by Franklin and others (2005) (fig. 4–8): (1) flow lithofacies association, (2) volcaniclastic lithofacies association, and (3) sedimentary lithofacies association (discussed under the "Relations to Sedimentary Rocks" section, this chapter). The associations can be further subdivided into mafic and felsic subtypes, based on the dominant composition of the volcanic rocks.

Flow Lithofacies Association

Flow-dominated successions include coherent ultramafic (komatiitic), mafic, and (or) felsic lava flows and domes and their associated autoclastic deposits (autobreccia, hyaloclastite, and their redeposited equivalents) (fig. 4–8). Synvolcanic intrusions are common and include dikes, sills, and occasionally cryptodomes (and associated peperite). Volcaniclastic rocks are a minor component and typically consist of redeposited hyaloclastite breccia and some primary pyroclastic deposits. Minor amounts of sedimentary rocks may be present and typically consist of carbonaceous argillite and immature volcanic-derived wacke, minor carbonate, and minor chemical sediments (exhalite, iron-formation).

Flow-dominated successions form volcanic complexes composed of single or composite submarine shield-like volcanoes constructed through effusive eruption processes at depths generally greater than 1,000 m (Gibson and others, 1999). In these successions, VMS deposits typically occur at breaks in volcanism, which can be marked by local or laterally extensive sulfidic, water-laid tuff, and (or) chemical sedimentary units (exhalite horizons). Because the host rocks are relatively impermeable, ascending hydrothermal fluids are focused along permeable zones and sulfide precipitation occurs at and immediately below the seafloor. Resulting regional semiconformable alteration is focused on areas of high permeability such as flow contacts, flow breccias, amygdules, and synvolcanic faults (Gibson and others, 1999). The sulfide deposits grow through the processes of chimney growth, collapse, replacement of chimney debris, and finally renewed chimney growth (Hannington and others, 1995) to form classic mound or lens-shaped deposits above a stringer or stockwork sulfide zone. Volcanogenic massive sulfide deposits that form in mafic flow-dominated successions tend to be Cu-rich, while those in felsic successions tend to be Cu-Zn±Pb-rich. Examples of VMS deposits in the flow lithofacies association include deposits forming on modern mid-ocean spreading ridges (Hannington and others, 1995), ophiolite-hosted deposits (Galley and Koski, 1999), and intracaldera deposits in the Archean Noranda Camp (Mueller and others, 2009).

Volcaniclastic Lithofacies Association

Volcaniclastic-dominated successions are largely composed of pyroclastic and syneruptive redeposited pyroclastic and epiclastic deposits, along with subordinate coherent mafic and felsic lava flows and domes (±autobreccia, hyaloclastite, and their redeposited equivalents), cryptodomes with associated peperite and (or) fluidal breccia, and lesser synvolcanic dikes, sills, and clastic sedimentary rocks (fig. 4–8). The clastic sedimentary rocks, which commonly occur within the hanging wall sequence, are typically carbonaceous argillite, immature epiclastic volcanic wacke, and carbonate units. The dominance of pyroclastic rocks in this lithofacies suggests explosive eruptions in relatively shallow (<1,000 m) water volcanic environments characterized by the construction of central volcanic complexes with one or more submarine volcanoes (Gibson and others, 1999). The occurrence of thick, localized successions of juvenile volcaniclastic rocks in the upper or central parts of the sequence suggests emplacement within large subsidence structures or calderas (Busby and

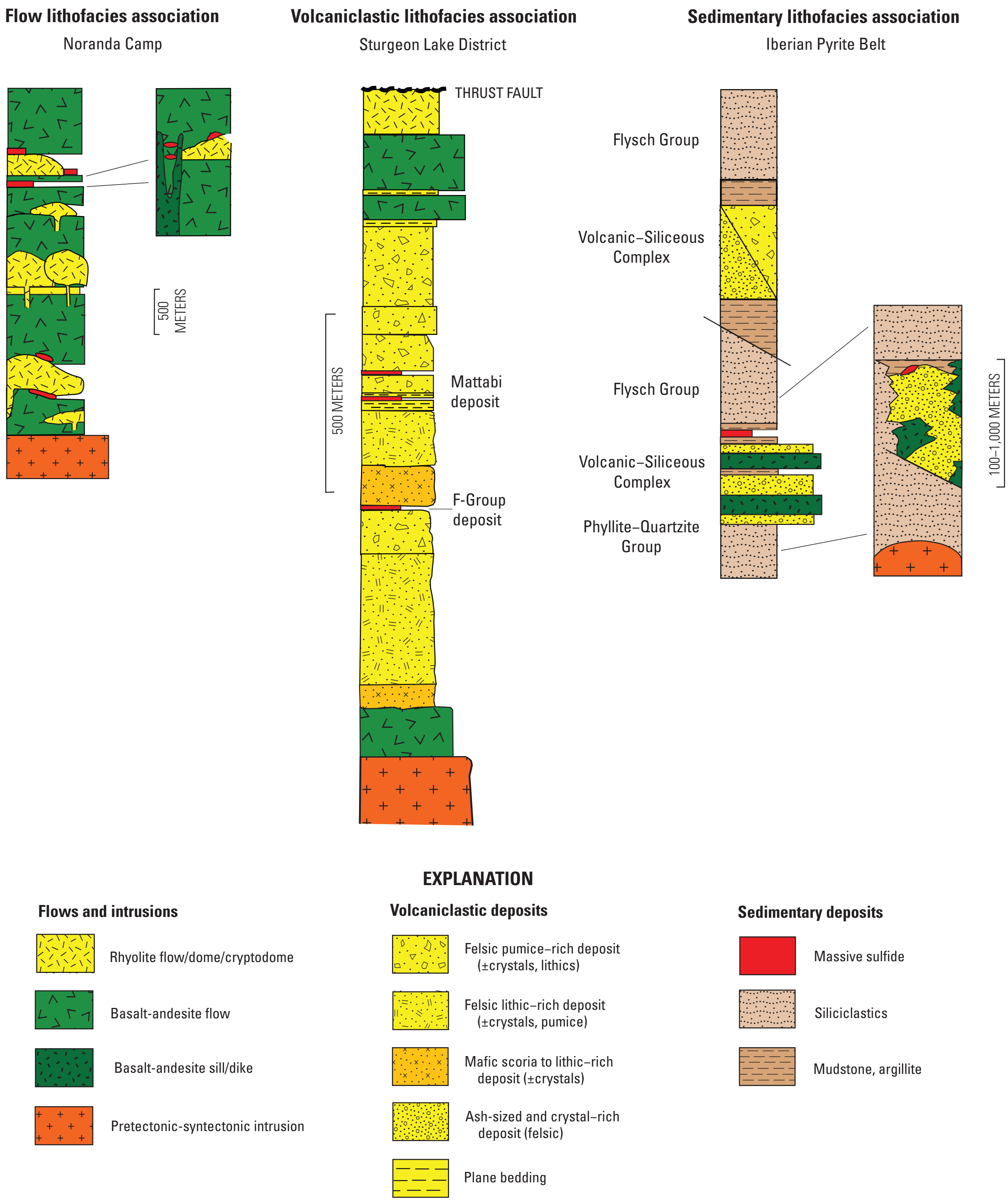

Figure 4–8. Composite stratigraphic sections illustrating flow, volcaniclastic, and sediment dominated lithofacies that host volcanogenic massive sulfide deposits. Modified from Franklin and others (2005).

others, 2003; Hudak and others, 2003; Mueller and others, 2009). Volcaniclastic lithofacies associations are common in bimodal-mafic, bimodal-felsic, and felsic-siliciclastic associations.

Initial hydrothermal discharge in volcaniclastic-dominated successions occurs over a larger area than in flow-dominated successions, with relatively unfocused discharge occurring from numerous coalescing hydrothermal vents that are sometimes confined to linear, fault-controlled depressions or grabens (Gibson and others, 1999). Sulfide precipitation commonly occurs within pore spaces of the highly permeable volcaniclastic footwall as unfocused ascending hydrothermal fluid is cooled by interaction with trapped and entrained seawater. This results in the replacement of the volcaniclastic rocks and formation of tabular or sheet-like, largely subseafloor replacement VMS deposits. With continued hydrothermal circulation, zone refining processes can lead to replacement of early-formed pyrite and pyrite-sphalerite mineralization by higher-temperature chalcopyrite and sphalerite-chalcopyrite assemblages (Eldridge and others, 1983). In addition, because some volcaniclastic-dominated successions develop in shallow water settings, the resulting VMS deposits may show similarities with subaerial epithermal deposits, including more Au-rich compositions and advanced argillic-type alteration zones, represented in ancient deposits by aluminum-silicate alteration assemblages or K-bearing assemblages (sericite, K-feldspar) (Gibson and others, 1999; Hannington and others, 1999e).

Examples of VMS deposits associated with volcaniclastic lithofacies association include the Horne, Gallen, and Mobrun deposits, Noranda Camp, Canada (Mueller and others, 2009); the Mattabi deposit, Sturgeon Lake Camp, Canada (Morton and others, 1991; Hudak and others, 2003); the Garpenberg and Zinkgruvan deposits, Bergslagen District, Sweden (Allen and others, 1996); the Rosebery and Hercules deposits, Tasmania (McPhie and Allen, 1992); and the Bald Mountain deposit, United States (Busby and others, 2003).

Relations to Sedimentary Rocks

Sediment-dominated successions that host VMS deposits consist of two distinct facies: (1) a siliciclastic facies composed predominantly of wacke, sandstone, siltstone, argillite, and locally iron formation or Fe-Mn-rich argillite, and (2) a pelitic facies with argillite, carbonaceous argillite, siltstone, marl, and carbonate (bioclastic and chemical) (Franklin and others, 2005). Also present in these sediment-dominated successions are subordinate coherent mafic and (or) felsic lava flows, domes, cryptodomes, and associated autobreccia, hyaloclastite, and peperite, or voluminous felsic volcaniclastic units with subordinate felsic lava flows, domes, and cryptodomes (fig. 4–8). In some sedimentary successions, the dominant volcanic component may be synvolcanic dikes, sills, and cryptodomes. The VMS deposits are spatially associated with complex volcanic centers developed in smaller subsidence structures located within larger sediment-filled extensional basins; however, the immediate host rocks may be either sedimentary or volcanic. Like some VMS deposits formed in volcaniclastic-dominated successions, deposits in sediment-dominated successions may form just below the seafloor through precipitation in pore spaces and replacement of the sedimentary rocks. This kind of formation may be aided by the presence of a cap layer of silica, carbonate, or sulfide acting as a physical barrier to ascending hydrothermal fluids. In sedimentary successions dominated by terrigenous clastic sedimentary rocks in continental rifts and back-arc basins, the VMS deposits generally contain significant Pb and Ag (Zn-Pb-Cu-Ag deposits) (Franklin and others, 2005). Ancient examples of VMS deposits in sediment-dominated successions include the Brunswick No. 12 deposit, Bathurst mining camp, Canada (Goodfellow and McCutcheon, 2003); Windy Craggy deposit, Canada (Peter and Scott, 1999); and deposits in the Iberian Pyrite Belt, Spain and Portugal (Carvalho and others, 1999).

Iron formations and other hydrothermally precipitated chemical sediments (for example, chert, jasper, Fe-Mn-rich sediment) commonly display a spatial and temporal association with VMS deposits (Spry and others, 2000) and are particularly well developed and laterally extensive in sediment-dominated successions that formed in continental rift and back-arc settings (for example, Bathurst mining camp, Canada). These “exhalites” typically occur in the immediate vicinity of the sulfide deposit and can be at the same stratigraphic horizon, or slightly lower or higher (Peter, 2003). Jaspers (hematitic cherts) commonly form thin, localized caps over VMS deposits, while in other districts relatively thin (<2 m thick) iron formations can form laterally extensive marker horizons that interconnect (in time and space) several massive sulfide deposits. These thinly bedded to laminated rocks are dominantly precipitated from submarine hydrothermal fluids, but they also contain contributions from clastic detritus (for example, Al, Ti) and seawater. Use of iron formation as a stratigraphic guide in the exploration for VMS deposits has met with variable success. A positive europium (Eu) anomaly in iron formation is taken to reflect high-temperature fluid venting and may serve as a guide to mineralization in some districts (Peter, 2003). In addition, mineralogical variations from oxide through carbonate to sulfide within regionally extensive iron formations may indicate proximity to more focused, higher temperature hydrothermal vent complexes (Galley and others, 2007), although subsequent metamorphism often overprints primary mineralogy.

Relations to Metamorphic Rocks

Volcanogenic massive sulfide deposits are syngenetic deposits and are not directly related to metamorphic processes. However, the stratified, district-scale semi-conformable alteration that typically develops from subseafloor hydrothermal convection above cooling sill complexes can produce alteration mineral assemblages that mimic those produced by regional metamorphism (Spooner and Fyfe, 1973; Alt, 1995; Hannington and others, 2003). The resulting alteration mineral assemblages can vary from amphibolite-facies assemblages (for example, Fe-Ca-rich amphibole, clinozoisite, Ca-plagioclase, magnetite) directly above the intrusions through Na-Ca-rich greenschist facies assemblages (for example, albite, quartz, chlorite, actinolite, epidote) to zeolite-clay and related subgreenschist facies mineral assemblages (for example, K-Mg-rich smectites, mixed-layer chlorites, K-feldspar) closer to the seafloor (Galley and others, 2007). In addition, some VMS deposits formed in shallow water settings are characterized by proximal aluminum silicate alteration of their footwall rocks. As described by Bonnet and Corriveau (2007), regional metamorphism of the hydrothermal alteration zones related to massive sulfide formation can produce distinctive mineral assemblages and rock types that can serve as guides to mineralization in ancient volcano-plutonic terranes (for example, hydrothermal aluminum silicate alteration can give rise to sillimanite-kyanite-quartz-biotite-cordierite-garnet assemblages at upper amphibolite-granulite metamorphism).

Prograde metamorphism of massive sulfides also produces changes (Marshall and others, 2000), including: (1) grain-size coarsening of the base metal sulfides; (2) conversion of pyrite to pyrrhotite and generation of pyrrhotite through sulfidation of Fe in other minerals above the greenschist-amphibolite facies boundary; (3) a progressive increase in the FeS content of sphalerite as well as chalcopyrite exsolution from sphalerite; (4) the formation of zinc spinel, zincian staurolite, and Pb-rich feldspar at upper amphibolite-granulite facies conditions; (5) the release of gold from pyrite and its partitioning between electrum and chalcopyrite; (6) release of other trace elements included or nonstoichiometrically substituted in base metal sulfides; and (7) the partitioning of trace elements between equilibrium sulfide pairs. Some of these prograde metamorphic effects can be reversed under appropriate retrograde processes (for example, pyrrhotite can undergo sulfidation to pyrite). In addition, deformation accompanying metamorphism can result in mobilization and redistribution of massive sulfide mineralization (Marshall and Gilligan, 1993; Marshall and others, 2000), including the separation of more ductile minerals, such as galena and sphalerite, from more brittle sulfide minerals, such as pyrite.

References Cited

Alabaster, T., and Pearce, J.A., 1985, The interrelationship between magmatic and ore-forming hydrothermal processes in the Oman ophiolite: Economic Geology, v. 80, p. 1–16.

Allen, R.L., Lundstrom, I., Ripa, M., Simeonov, A., and Christofferson, H., 1996, Facies analysis of a 1.9 Ga continental margin, back-arc, felsic province with diverse Zn-Pb-Ag (Cu-Au) sulfide and Fe oxide deposits, Bergslagen Region, Sweden: Economic Geology, v. 91, p. 979–1008.

Allen, R.L., Weihed, P., and Team, G.V.R.P., 2002, Global comparisons of volcanic-associated massive sulphide districts, *in* Blundell, D.J., Neubauer, F., and Von Quadt, A., eds., The Timing and Location of Major Ore Deposits in an Evolving Orogen: Geological Society, London, Special Publication 204, p. 13–37.

Alt, J.C., 1995, Subseafloor processes in mid-ocean ridge hydrothermal systems, *in* Humphris, S.E., Zierenberg, R.A., Mullineaux, L.S., and Thomas, R.E., eds., Seafloor hydrothermal systems—Physical, chemical, biological, and geological interactions: American Geophysical Union, Geophysical Monograph 91, p. 85–114.

Baker, E.T., 2009, Relationships between hydrothermal activity and axial magma chamber distribution, depth, and melt content: Geochemistry Geophysics Geosystems, v. 10, Q06009, 15 p., doi.10.1029/2009GC002424.

Baker, E.T., and German, C.R., 2004, On the global distribution of hydrothermal vent sites, *in* Lowell, R.P., Seewald, J., Metaxa, A., and Perfit, M., eds., Magma to Microbe—Modeling Hydrothermal Processes at Oceanic Spreading Centers: American Geophysical Union Geophysical Monograph 148, p. 1–18.

Baker, E.T., Chen, Y.J., and Phipps Morgan, J., 1996, The relationship between near-axis hydrothermal cooling and the spreading rate of mid-ocean ridges: Earth and Planetary Science Letters, v. 142, p. 137–145.

Barley, M.E., and Groves, D.I., 1992, Supercontinent cycles and the distribution of metal deposits through time: Geology, v. 20, p. 291–294.

Barrett, T.J., and MacLean, W.H., 1999, Volcanic sequences, lithogeochemistry, and hydrothermal alteration in some bimodal volcanic-associated massive sulfide deposits, *in* Barrie, C.T., and Hannington, M.D., eds., Volcanic-associated massive sulfide deposits—Processes and examples in modern and ancient settings: Reviews in Economic Geology, v. 8, p. 101–131.

Barrett, T.J., and Sherlock, R.L., 1996, Geology, lithogeochemistry and volcanic setting of the Eskay Creek Au-Ag-Cu-Zn deposit, northwestern British Columbia: Exploration and Mining Geology, v. 5, p. 339–368.

Barrett, T.J., Thompson, J.F.H., and Sherlock, R.L., 1996, Stratigraphic, lithogeochemical and tectonic setting of the Kutcho Creek massive sulfide deposit, northwestern British Columbia: Exploration and Mining Geology, v. 5, p. 309–338.

Barrie, C.T., Hannington, M.D., and Bleeker, W., 1999, The giant Kidd Creek volcanic-associated massive sulfide deposit, Abitibi Subprovince, Canada, *in* Barrie, C.T., and Hannington, M.D., eds., Volcanic-associated massive sulfide deposits—Processes and examples in modern and ancient settings: Reviews in Economic Geology, v. 8, p. 247–259.

Bédard, J.H., and Hébert, R., 1996, The lower crust of the Bay of Islands ophiolite in Canada—Petrology, mineralogy, and the importance of syntexis in magmatic differentiation in ophiolites and at ocean ridges: Journal of Geophysical Research, v. 101, p. 25,105–25,124.

Binney, W.P., 1987, A sedimentological investigation of Maclean channel transported sulfide ores, *in* Kirkham, R.V., ed., Buchans geology, Newfoundland: Geological Survey of Canada Paper 86-24, p. 107–147.

Bogdanov, Y.A., Bortnikov, N.S., Vikent'ev, I.V., Gurvich, E.G., and Sagalevich, A.M., 1997, A new type of modern mineral-forming systems—Black smokers of the hydrothermal field at 14°45'N latitude, Mid-Atlantic Ridge: Geology of Ore Deposits, v. 39, p. 68–90.

Bonnet, A-L., and Corriveau, L., 2007, Alteration vectors to metamorphosed hydrothermal systems in gneissic terranes, *in* Goodfellow, W.D., ed., Mineral Resources of Canada—A Synthesis of Major Deposit-Types, District Metallogeny, the Evolution of Geological Provinces, and Exploration Methods: Geological Association of Canada, Mineral Deposits Division, Special Publication No. 5, p. 1035–1050.

Busby, C.J., Kessel, L., Schulz, K.J., Foose, M.P., and Slack, J.F., 2003, Volcanic setting of the Ordovician Bald Mountain massive sulfide deposit, northern Maine, *in* Goodfellow, W.D., McCutcheon, S.R., and Peter, J.M., eds., Volcanogenic massive sulfide deposits of the Bathurst district, New Brunswick, and northern Maine: Economic Geology Monograph 11, p. 219–244.

Carr, P.M., and Cathless, L.M., III, 2008, On the size and spacing of volcanogenic massive sulfide deposits within a district with application to the Matagami District, Quebec: Economic Geology, v. 103, p. 1395–1409.

Carvalho, D., Barriga, F.J.A.S., and Munhá, J., 1999, Bimodal siliciclastic systems—The case of the Iberian Pyrite Belt, *in* Barrie, C.T., and Hannington, M.D., eds., Volcanic-associated massive sulfide deposits—Processes and examples in modern and ancient settings: Reviews in Economic Geology, v. 8, p. 375–408.

Clift, P.D., and ODP Leg 135 Scientific Party, 1994, Volcanism and sedimentation in a rifting island-arc terrain: An example from Tonga, SW Pacific, *in* Smellie, J.L., ed., Volcanism Associated with Extension at Consuming Plate Margins: Geological Society, London, Special Publication 81, p. 29–51.

Condie, K.C., and Pease, V., editors, 2008, When did plate tectonics begin on planet Earth?: Geological Society of America Special Paper 440, 294 p.

Coumou, D., Driesner, T., and Heinrich, C.A., 2008, The structure and dynamics of mid-ocean ridge hydrothermal systems: Science, v. 321, p. 1825–1828.

Cox, S.F., Knackstedt, M.A., and Braun, J., 2001, Principles of structural control on permeability and fluid flow in hydrothermal systems: Reviews in Economic Geology, v. 14, p. 1–24.

Crawford, W.C., Hildebrand, J.A., Dorman, L.M., Webb, S.C., and Wiens, D.A., 2003, Tonga Ridge and Lau Basin crustal structure from seismic refraction data: Journal of Geophysical Resaerch, v. 108(B4), 2195, 19 p., doi:10.1029/2001JB001435.

Crowe, D.E., Nelson, S.W., Brown, P.E., Shanks, W.C., III, and Valley, J.W., 1992, Geology and geochemistry of volcanogenic massive sulfide deposits and related igneous rocks, Prince William Sound, south-central Alaska: Economic Geology, v. 87, p. 1,722–1,746.

Curewitz, D., and Karson, J.A., 1997, Structural settings of hydrothermal outflow—Fracture permeability maintained by fault propagation and interaction: Journal of Volcanology and Geothermal Research, v. 79, p. 149–168.

de Ronde, C.E.J., 1995, Fluid chemistry and isotopic characteristics of seafloor hydrothermal systems and associated VMS deposits: potential for magmatic contributions, *in* Thompson, J.F.H., ed., Magmas, fluids and ore deposits: Ottawa, Ontario, Mineralogical Association of Canada Short Course Series, p. 479–510.

de Ronde, C.E.J., Massoth, G.J., Baker, E.T., and Lupton, J.E., 2003, Submarine hydrothermal venting related to volcanic arcs, *in* Simmons, S.F., and Graham, I.J., eds., Volcanic, geothermal and ore-forming fluids: Rulers and witnesses of processes within the Earth: Society of Economic Geologists Special Publication 10, p. 91–109.

de Ronde, C.E.J., Baker, E.T., Massoth, G.J., Lupton, J.E., Wright, I.C., Sparks, R.J., Bannister, S.C., Reyners, M.E., Walker, S.L., Greene, R.R., Ishibashi, J., Faure, K., Resing, J.A., and Lebon, G.T., 2007, Submarine hydrothermal activity along the mid-Kermadec Arc, New Zealand—Large-scale effects on venting: Geochemistry, Geophysics, Geosystems, v. 8, Q07007, 27 p., doi:10.1029/2006GC001495.

Delaney, J.R., Robigou, V., McDuff, R.E., and Tivey, M.K., 1992, Geology of a vigorous hydrothermal system on the Endeavour segment, Juan de Fuca Ridge: Journal of Geophysical Research, v. 97, p. 19,663–19,682.

DeMatties, T.A., 1994, Early Proterozoic volcanogenic massive sulfide deposits in Wisconsin: An overview: Economic Geology, v. 89, p. 1122–1151.

Dusel-Bacon, C., Wooden, J.L., and Hopkins, M.J., 2004, U-Pb zircon and geochemical evidence for bimodal mid-Paleozoic magmatism and syngenetic base-metal mineralization in the Yukon-Tanana terrane, Alaska: Geological Society of America Bulletin, v. 116, p. 989–1015.

Einsele, G., 1985, Basaltic sill-sediment complexes in young spreading centers—Genesis and significance: Geology, v. 13, p. 249–252.

Eldridge, C.S., Barton, P.B., and Ohomoto, H., 1983, Mineral textures and their bearing on the formation of the Kuroko orebodies, *in* Ohmoto, H., and Skinner, B.J., eds., The Kuroko and related volcanogenic massive sulfide deposits: Economic Geology Monograph 5, p. 241–281.

Escartin, J., Smith, D.K., Cann, J., Schouten, H., Langmuir, C.H., and Escrig, S., 2008, Central role of detachment faults in accretion of slow-spreading oceanic lithosphere: Nature, v. 455, p. 790–795.

Ewart, A., Collerson, K.D., Regelous, M., Wendt, J.I., and Niu, Y., 1998, Geochemical evolution within the Tonga-Kermadec-Lau arc-back-arc systems—The role of varying mantle wedge composition in space and time: Journal of Petrology, v. 39, p. 331–368.

Fiske, R.S., Cashman, C.V., Shibata, A., and Watanabe, K., 1998, Tephra dispersal from Myojinsho, Japan, during it shallow submarine eruption of 195201953: Bulletin of Volcanology, v. 59, p. 262–275.

Fiske, R.S., Naka, J., Iizasa, K., Yuasa, M., and Klaus, A., 2001, Submarine silicic caldera at the front of the Izu-Bonin Arc, Japan—Voluminous seafloor eruptions of rhyolite pumice: Geological Society of America Bulletin, v. 113, p. 813–824.

Francheteau, J., Needham, H.D., Choukroune, P., Juteau, J., Seguret, M., Ballard, R.D., Fox, P.J., Normark, W., Carranza, A., Cordoba, A., Guerrero, j., Rangin, C., Bougault, H., Cambon, P., and Hekinina, R., 1979, Massive deep sea sulfide ore deposit discovered on the East Pacific Rise: Nature, v. 277, p. 523–528.

Franklin, J.M., Gibson, H.L., Jonasson, I.R., and Galley, A.G., 2005, Volcanogenic massive sulfide deposits, *in* Hedenquist, J.W., Thompson, J.F.H., Goldfarb, R.J., and Richards, J.P., eds., Economic Geology 100th anniversary volume, 1905–2005: Littleton, Colo., p. 523–560.

Galley, A.G., 1993, Characteristics of semi-conformable alteration zones associated with volcanogenic massive sulphide districts: Journal of Geochemical Exploration, v. 48, p. 175–200.

Galley, A.G., 2003, Composite synvolcanic intrusions associated with Precambrian VMS-related hydrothermal systems: Mineralium Deposita, v. 38, p. 443–473.

Galley, A.G., and Koski, R.A., 1999, Setting and characteristics of ophiolite-hosted volcanogenic massive sulfide deposits, *in* Barrie, C.T., and Hannington, M.D., eds., Volcanic-Associated Massive Sulfide Deposits—Processes and Examples in Modern and Ancient Settings, p. 215–236.

Galley, A.G., Hannington, M.D., and Jonasson, I.R., 2007, Volcanogenic Massive Sulphide Deposits, *in* Goodfellow, W.D., ed., Mineral deposits of Canada—A synthesis of major deposit-types, district metallogeny, the evolution of geological provinces, and exploration methods: Geological Association of Canada, Mineral Deposits Division, Special Publication No. 5, p. 141–161.

Gibson, H.L., and Galley, A.G., 2007, Volcanogenic massive sulphide deposits of the Archean, Noranda district, Quebec, *in* Goodfellow, W.D., ed., Mineral deposits of Canada—A synthesis of major deposit-types, district metallogeny, the evolution of geological provinces, and exploration methods: Geological Association of Canada, Mineral Deposits Division, Special Publication No. 5, p. 533–552.

Gibson, H.L., Morton, R.L., and Hudak, G.J., 1999, Submarine volcanic processes, deposits and environments favorable for the location of volcanic-associated massive sulfide deposits, *in* Barrie, C.T., and Hannington, M.D., eds., Volcanic-associated massive sulfide deposits—Processes and examples in modern and ancient settings: Reviews in Economic Geology, v. 8, p. p.13–51.

Goodfellow, W.D., and McCutcheon, S.R., 2003, Geologic and genetic attributes of volcanic sediment-hosted massive sulfide deposits of the Bathurst Mining Camp, northern New Brunswick—A synthesis, *in* Goodfellow, W.D., McCutcheon, S.R., and Peter, J.M., eds., Massive sulfide deposits of the Bathurst Mining Camp, New Brunswick, and northern Maine: Economic Geology Monograph 11, p. 79–109.

Graham, I.J., Reyes, A.G., Wright, I.C., Peckett, K.M., Smith, I.E.M., and Arculus, R.J., 2008, Structure and petrology of newly discovered volcanic centers in the northern Kermadec-southern Tofa arc, South Pacific Ocean: Journal of Geophysical Research, v. 113, B08S02, 24 p., doi:10.1029/2007JB005453.

Grenne, T., 1989, The feeder-zone to the Lokken ophiolite-hosted massive sulphide deposit and related mineralizations in the central Norwegian Caledonides: Economic Geology, v. 84, p. 2173–2195.

Groves, D.I., and Bierlein, F.P., 2007, Geodynamic settings of mineral deposit systems: Journal of the Geological Society of London, v. 164, p. 19–30.

Groves, D.I., Vielreicher, R.M., Goldfarb, R.J., and Condie, K.C., 2005, Controls on the heterogeneous distribution of mineral deposits through time, *in* MacDonald, I., Boyce, A.J., Butler, I.B., Herrington, R.J., and Polya, D., eds., Mineral deposits and earth evolution: Geological Society of London, Special Publication 248, p. 71–101.

Halbach, P., Nakamura, K., Washner, M., Lange, J., Sakai, H., Kaselitz, L., Hansen, R-D., Yamano, M., Post, J., Prause, B., Seifert, R., Michaelis, W., Teichmann, F., Kinoshita, M., Marten, A., Ishibashi, J., Czerwinski, S., and Blum, N., 1989, Probable modern analogue of Kuroko-type massive sulfide deposits in the Okinawa trough back-arc basin: Nature, v. 338, p. 496–499.

Halbach, P., Pracejus, B., and Marten, A., 1993, Geology and mineralogy of massive sulfide ores from the central Okinawa trough: Economic Geology, v. 88, p. 2,210–2,225.

Hannington, M.D., de Ronde, C.E., and Petersen, S., 2005, Sea-floor tectonics and submarine hydrothermal systems, *in* Hedenquist, J.W., Thompson, J.F.H., Goldfarb, R.J., and Richards, J.P., eds., Economic Geology 100th anniversary volume, 1905–2005: Littleton, Colo., p. 111–141.

Hannington, M.D., Jonasson, I.R., Herzig, P.M., and Petersen, S., 1995, Physical and chemical processes of seafloor mineralization at Mid-Ocean Ridges, *in* Humphris, S.E., Zierenberg, R.A., Mullineaux, L.S., and Thomas, R.E., eds., Seafloor hydrothermal systems—Physical, chemical, biological, and geological interactions: American Geophysical Union, Geophysical Monograph 91, p. 115–157.

Hannington, M.D., Petersen, S., Herzig, P.M., and Jonnasson, I.R., 2004, A global database of seafloor hydrothermal systems, including a digital database of geochemical analyses of seafloor polymetallic sulfides: Geological Survey of Canada Open File 4598, CD-ROM.

Hannington, M.D., Poulsen, K.H., Thompson, J.F.H., and Sillitoe, R.H., 1999, Volcanogenic gold in the massive sulfide environment, *in* Barrie, C.T., and Hannington, M.D., eds., Volcanic-associated massive sulfide deposits—Processes and examples in modern and ancient settings: Reviews in Economic Geology, v. 8, p. 325–356.

Hannington, M.D., Santaguida, F., Kjarsgaard, I.M., and Cathless, L.M., 2003, Regional greenschist facies hydrothermal alteration in the central Blake River Group, western Abitibi subprovince, Canada: Mineralium Deposita, v. 38, 393–422.

Hart, T.R., Gibson, H.L., and Lesher, C.M., 2004, Trace element geochemistry and petrogenesis of felsic volcanic rocks associated with volcanogenic massive Cu-Zn-Pb sulfide deposits: Economic Geology, v. 99, p. 1003–1013.

Haymon, R.M., Fornari, D.J., Edwards, M.H., Carbotte, S., Wright, D., and MacDonald, K.C., 1991, Hydrothermal vent distribution along the East Pacific Rise crest (9°09' - 54'N) and its relationship to magmatic and tectonic processes on fast-spreading mid-ocean ridges: Earth and Planetary Sciences, v. 104, p. 513–534.

Hawkins, J.W., Jr., 1995, The geology of the Lau basin, in Taylor, B., ed., Backarc Basins—Tectonics and magmatism: New York, Plenum Press, p. 63–138.

Heiken, G., Goff, F., Stix, J., Tamanyu, S., Shafiqullah, M., Garcia, S., and Hagan, R., 1986, Intracaldera volcanic activity, Toledo caldera and embayment, Jemez Mountains, New Mexico: Journal of Geophysical Research, v. 91, p. 1799–1815.

Hofmann, A.W., 2003, Sampling mantle heterogeneity through oceanic basalts—Isotopes and trace elements: Treatise on Geochemistry, v. 2, p. 61–101.

Hudak, G.J., Mortan, R.L., Franklin, J.M., and Peterson, D.M., 2003, Morphology, distribution, and estimated eruption volumes for intracaldera tuffs associated with volcanic-hosted massive sulfide deposits in the Archean Sturgeon Lake Caldera Complex, Northwestern Ontario, *in* White, J.D.L., Smellie, J.L., and Clague, D.A., eds., Explosive subaqueous volcanism: American Geophysical Union, Geophysical Monograph 140, p. 345–360.

Humphris, S.E., and Tivey, M.K., 2000, A synthesis of geological and geochemical investigations of the TAG hydrothermal field: Insights into fluid flow and mixing processes in a hydrothermal system, *in* Dilek, Y., Moorse, E., Elthon, D., and Nicholas, A., eds., Ophiolites and oceanic crust—New insights from field studies and the ocean drilling program: Geological Society of America Special Paper 349, p. 213–236.

Iizasa, K., Fiske, R.S., Ishizuka, O., Yuasa, M., Hashimoto, J., Ishibashi, J., Naka, J., Horii, Y., Fujiwara, Y., Imai, A., and Koyama, S., 1999, A Kuroko-type polymetallic sulfide deposit in a submarine caldera: Science, v. 283, p. 975–977.

Ishibashi, J., and Urabe, T., 1995, Hydrothermal activity related to arc-backarc magmatism in the Western Pacific, in Taylor, B., ed., Backarc basins—Tectonics and magmatism: New York, Plenum Press, p. 451–495.

Johnson, B.J., Montante-Martínez, J.A., Canela-Barboza, M., and Danielson, T.J., 2000, Geology of the San Nicolás deposit, Zacatecas, Mexico, *in* Sherlock, R.L., and Logan, M.A.V., eds., Volcanogenic massive sulphide deposits of Latin America: Geological Association of Canada, Mineral Deposits Division Special Publication 2, p. 71–85.

Kelley, D.S., Delaney, J.R., and Yoerger, D.A., 2001, Geology and venting characteristics of the Mothra hydrothermal field, Endeavour segment, Juan de Fuca Ridge: Geology, v. 29, p. 385–491.

Kennedy, B., Stix, J., Vallance, J.W., Lavallée, Y., and Longpré, M-A., 2004, Controls on caldera structure—Results from analogue sandbox modeling: Geological Society of America Bulletin, v. 116, p. 515–524.

Kleinrock, M.C., and Humphris, S.E., 1996, Structural control on sea-floor hydrothermal activity at the TAG active mound: Nature, v. 382, p. 149–153.

Kleinrock, M.C., Tucholke, B.E., Lin, J., and Tivey, M.A., 1997, Fast rift propagation at a slow-spreading ridge: Geology, v. 25, p. 639–642.

Kodaira, S., Sato, T., Takahashi, N., Miura, S., Tamura, Y., Tatsumi, Y., and Kaneda, Y., 2007, New seismological constraints on growth of continental crsut in the Izu-Bonin intra-oceanic arc: Geology, v. 35, p. 1031–1034.

Krasnov, S.G., Proroshina, I.M., and Cherkashev, G.A., 1995, Geological setting of high-temperature hydrothermal activity and massive sulfide formation on fast and slow-spreading ridges, *in* Parson, L.M., Walker, C.L., and Dixon, D.R., eds., Hydrothermal Vents and Processes: Geological Society of London, Special Publication 87, p. 17–32.

Knuckey, M.J., Comba, C.D.A., and Riverin, G., 1982, Structure, metal zoning and alteration at the Millenbach deposit, Noranda, Quebec, *in* Hutchinson, R.W., Spence, C.D., and Franklin, J.M., eds., Precambrian sulphide deposits: Geological Association of Canada Special Paper 25, p. 255–295.

Lalou, C., Reyss, J-L., Brichet, E., Rona, P.A., and Thompson, G., 1995, Hydrothermal activity on a 10^5-year scale at a slow-spreading ridge, TAG hydrothermal field, Mid-Atlantic Ridge 26°N: Journal of Geophysical Research, v. 100, p. 17855–17862.

Large, R.R., 1992, Australian volcanic-hosted massive sulfide deposits: Features, styles, and genetic models: Economic Geology, v. 87, p. 471–510.

Lentz, D.R., 1998, Petrogenetic evolution of felsic volcanic sequences associated with Phanerozoic volcanic-hosted massive sulfide systems—The role of extensional geodynamics: Ore Geology Reviews, v. 12, p. 289–327.

Lonsdale, P., 1989, Geology and tectonic history of the Gulf of California, *in* Winterer, E.L., Hussong, D.M., and Decker, R.W., eds., The Eastern Pacific Ocean and Hawaii: Geological Society of America, Decade of North America Geology, v. N, p. 499–521.

Lonsdale, P., and Becker, K., 1985, Hydrothermal plumes, hot springs, and conductive heat flow in the Southern Trough of Guaymas Basin: Earth and Planetary Sciences, v. 73, p. 211–225

Marsaglia, K.M., 1995, Interarc and backarc basins, *in* Busby, C.J., and Ingersoll, R.V., eds., Tectonics of sedimentary basins: Cambridge, Mass., Blackwell Science, p. 299–329.

Marshall, B., and Gilligan, L.B., 1993, Remobilization, syn-tectonic processes and massive sulfide deposits: Ore Geology reviews, v. 8, p. 39–64.

Marshall, B., Vokes, F.M., and Larocque, A.C.L., 2000, Regional metamorphic remobilization: Upgrading and formation of ore deposits, *in* Spry, P.G., Marshall, B., and Vokes, F.M., eds., Metamorphosed and metamorphic ore deposits: Reviews in Economic Geology, v. 11, p. 19–38.

McCaig, A.M., Cliff, R.A., Escartin, J., Fallick, A.E., and MacLeod, C.J., 2007, Oceanic detachment faults focus very large volumes of black smoker fluids: Geology, v. 35, p. 935–938.

McPhie, J., and Allen, R.L., 1992, Facies architecture of mineralized submarine volcanic sequences: Cambrian Mount Read Volcanics, Western Tasmania: Economic Geology, v. 87, p. 587–596.

Morton, R.L., Walker, J.S., Hudak, G.J., and Franklin, J.M., 1991, The early development of an Archean submarine caldera complex with emphasis on the Mattabi ash-flow tuff and its relationship to the Mattabi massive sulfide deposit: Economic Geology, v. 86, p. 1002–1011.

Mosier, D.L., Berger, V.I., and Singer, D.A., 2009, Volcanogenic massive sulfide deposits of the world—Database and grade and tonnage models: U.S. Geological Survey Open-File Report 2009–1034, 46 p.

Mueller, W.U., and Mortensen, J., 2002, Age constraints and characteristics of subaqueous volcanic construction, the Archean Hunter Mine Group, Abitibi greenstone belt: Precambrian Research, v. 115, p. 119–152.

Mueller, W.U., Stix, J., Corcoran, P.I., and Daigneault, R., 2009, Subaqueous calderas in the Archean Abitibi greenstone belt: An overview and new ideas: Ore Geology Reviews, v. 35, p. 4–46.

Mumin, A.H., Scott, S.D., Somarin, A.K., and Oran, K.S., 2007, Structural controls on massive sulfide deposition and hydrothermal alteration in the South Sturgeon Lake caldera, Northwestern Ontario: Exploration and Mining Geology, v. 16, p. 83–107.

Ohmoto, H., 1978, Submarine calderas: A key to the formation of volcanogenic massive sulfide deposits: Mining Geology, v. 28, p. 219–231.

Ohmoto, H., and Skinner, B.J., eds., 1983, The Kuroko and related volcanogenic massive sulfide deposits: Economic Geology Monograph 5, 604 pp.

Ohmoto, H., and Takahashi, T., 1983, Part III. Submarine calderas and Kuroko genesis, *in* Ohmoto, H., and Skinner, B.J., eds., The Kuroko and related volcanogenic massive sulfide deposits: Economic Geology Monograph 5, p. 39–54.

Pearce, J.A., 2003, Supra-subduction zone ophiolites: The search for modern analogues, *in* Dilek, Y., and Newcomb,S., eds., Ophiolite concept and the evolution of geological thought: Geological Society of America Special Paper 373, p. 269–293.

Pearce, J.A., and Peate, D.W., 1995, Tectonic implications of the composition of volcanic arc magmas: Annual Review of Earth and Planetary Sciences, v. 23, p. 251–285.

Pearce, J.A., and Stern, R.J., 2006, Origin of back-arc basin magmas: Trace element and isotope perspective, *in* Christie, D.M., Fisher, C.R., Lee, S-M, and Givens, S., eds., Back-arc spreading systems—Geological, Biological, Chemical, and Physical Interactions: American Geophysical Union Geophysical Monograph 166, p. 63–86.

Pearson, V., and Daigneault, R., 2009, An Archean megacaldera complex—The Blake River Group, Abitibi greenstone belt: Precambrian Research, v. 168, p. 66–82.

Perfit, M.R., Ridley, W.I., and Jonasson, I.R., 1999, Geologic, petrologic, and geochemical relationships between magmatism and massive sulfide mineralization along the eastern Galapagos spreading center, *in* Barrie, C.T., and Hannington, M.D., eds., Volcanic-associated massive sulfide deposits—Processes and examples in modern and ancient settings: Reviews in Economic Geology, v. 8, p. 75–100.

Perk, N.W., Coogan, L.A., Karson, J.A., Klein, E.M., and Hanna, H.D., 2007, Petrology and geochemistry of primitive lower oceanic crust from Pito Deep—Implications for the accretion of the lower crust at the Southern East Pacific Rise: Contributions to Mineralogy and Petrology, v. 154, p. 575–590.

Peter, J.M., 2003, Ancient iron-rich metalliferous sediments (iron formations): Their genesis and use in exploration for strataform base metal sulphide deposits, with examples from the Bathurst Mining Camp, *in* Lentz, D.R., ed., Geochemistry of sediments and sedimentary rocks—Evolutionary considerations to mineral deposit-forming environments: Geological Association of Canada, GEOtext 4, p. 145–173.

Peter, J.M., and Scott, S.D., 1999, Windy Craggy, northwestern British Columbia: The world's largest Besshi-type deposit, *in* Barrie, C.T., and Hannington, M.D., eds., Volcanic-associated massive sulfide deposits—Processes and examples in modern and ancient settings: Reviews in Economic Geology, v. 8, p. 261–295.

Petersen, S., Herzig, P.M., and Hannington, M.D., 2000, Third dimension of a presently forming VMS deposit: TAG hydrothermal mound, Mid-Atlantic Ridge, 26°N: Mineralium Deposita, v. 35, p. 233–259.

Rona, P.A., Hannington, M.D., Raman, C.V., Thompson, G., Tivey, M.K., Humphris, S., and Lalou, C., 1993, Active and relict seafloor hydrothermal mineralization at the TAG hydrothermal field, Mid Atlantic Ridge: Economic Geology, v. 88, p. 1989–2017.

Sangster, D.F., 1980, Quantitative characteristics of volcanogenic massive sulphide deposits—Part I. Metal content and size distribution of massive sulphide deposits in volcanic centres: Canadian Institute of Mining and Metallurgy Bulletin, v. 73, no. 814, p. 74–81.

Sangster, A.L., Douma, S.L., and Lavigne, J., 2007, Base metal and gold deposits of the Betts Cove Complex, Baie Verte Peninsula, Newfoundland, *in* Goodfellow, W.D., ed., Mineral deposits of Canada—A synthesis of major deposit-types, district metallogeny, the evolution of geological provinces, and exploration methods: Geological Association of Canada, Mineral Deposits Division, Special Publication 5, p. 703–721.

Schardt, C., and Large, R.R., 2009, New insights into the genesis of volcanic-hosted massive sulfide deposits on the seafloor from numerical modeling studies: Ore Geology Reviews, v. 35, p. 333–351.

Schmincke, H.-U., 2004, Volcanism: Berlin, Springer, 324 p.

Schulz, K.J., and Ayuso, R.A., 2003, Lithogeochemistry and paleotectonic setting of the Bald Mountain massive sulfide deposit, northern Maine, *in* Goodfellow, W.D., McCutcheon, S.R., and Peter, J.M., eds., Massive sulfide deposits of the Bathurst Mining Camp, New Brunswick, and northern Maine: Economic Geology Monograph 11, p. 79–109.

Scott, S.D., 1980, Geology and structural control of Kuroko-type massive sulfide deposits: Geological Association of Canada Special Paper 20, p. 705–721.

Scott, S.D., 1997, Submarine hydrothermal systems and deposits, in Barnes, H.L., ed., Geochemistry of hydrothermal ore deposits: New York, Wiley and Sons, p. 797–875.

Sharpe, R., and Gemmell, J.B., 2002, The Archean Cu-Zn magnetite-rich Gossan Hill volcanic-hosted massive sulfide deposit, Western Australia—Genesis of a multistage hydrothermal system: Economic Geology, v. 97, p. 517–539.

Shinjo, R., and Kato, Y., 2000, Geochemical constraints on the origin of bimodal magmatism at the Okinawa trough, and incipient back-arc basin: Lithos, v. 54, p. 117–137.

Sibuet, J.-C., Hsu, S.-K., Shyn, C.-T., and Liu, C.-S., 1995, Structural and kinematic evolution of the Okinawa trough backarc basin, *in* Taylor, B., ed., Backarc basins—Tectonics and Magmatism: New York, Plenum Press, p. 343–378.

Sinha, M.C., and Evans, R.L., 2004, Geophysical constraints upon the thermal regime of ocean crust, *in* German, C.R., and others, eds., Mid-ocean ridges—Hydrothermal interactions between the lithosphere and oceans: American Geophysical Union Geophysical Monograph 148, p. 19–62.

Slack, J.F., 1993, Descriptive and grade-tonnage models for Besshi-type massive sulfide deposits, *in* Kirkham, R.V., Sinclair, W.D., Thorpe, R.I., and Duke, J.M., eds., Mineral deposit models: Geological Association of Canada Special Paper 40, p. 343–371.

Slack, J.F., Foose, M.P., Flohr, M.J.K., Scully, M.V., and Belkin, H.E., 2003, Exhalative and subseafloor replacement processes in the formation of the Bald Mountain massive sulfide deposit, northern Maine, *in* Goodfellow, W.D., McCutcheon, S.R., and Peter, J.M., eds., Volcanogenic massive sulfide deposits of the Bathurst district, New Brunswick, and northern Maine: Economic Geology Monograph 11, p. 513–548.

Smith, D.K., Escartin, J., Schouten, H., and Cann, J.R., 2008, Fault rotation and core complex formation—Significant processes in seafloor formation at slow-spreading mid-ocean ridges (Mid-Atlantic Ridge, 13°-15°N): Geology Geophysics Geosystems, v. 9, Q03003, 23 p., doi:10.1029/2007GC001699.

Smith, I.E.M., Worthington, T.J., Stewart, R.B., Price, R.C., and Gamble, J.A., 2003, Felsic volcanism in the Kermadec arc, SW Pacific—Crustal recycling in an oceanic setting, *in* Larter, R.D., and Leet, P.T., eds., Intra-oceanic subduction systems—Tectonic and magmatic processes: Geological Society of London, Special Publication 219, p. 99–118.

Smith, R.L., 1979, Ash-flow magmatism, in Chapin, C.E., and Elston, W.E., eds., Ash-flow tuffs: Geological Society of America Special Paper 180, p. 5–27.

Solomon, M., 2008, Brine pool deposition for the Zn-Pb-Cu massive sulphide deposits of the Bathurst mining camp, New Brunswick, Canada. I. Comparisons with the Iberian pyrite belt: Ore Geology Reviews, v. 33, p. 329–351.

Spiess, F.N., Macdonald, K.C., Atwater, T., Ballard, R., Carranza, A., Cordoba, D., Cox, C., Diaz Garcia, V.M., Francheteau, J., Guerrero, J., Hawkins, J., Haymon, R., Hessler, R., Juteau, T., Kastner, M., Larson, R., Luyendyk, B., Macdougall, J.D., Miller, S., Normark, W., Orcutt, J., and Rangin, C., 1980, East Pacific Rise—Hot springs and geophysical experiments: Science, v. 207, no. 4438, p. 1421–1433.

Spooner, E.T.C., and Fyfe, W.S., 1973, Subseafloor metamorphism, heat and mass transfer: Contribution to Mineralogy and Petrology, v. 42, p. 287–304.

Spry, P.G., Peter, J.M., and Slack, J.F., 2000, Meta-exhalites as exploration guides to ore, in Spry, P.G., Marshall, B., and Vokes, F.M., eds., Metamorphosed and metamorphic ore deposits: Reviews in Economic Geology, v. 11, p. 163–201.

Stern, R.J., and Bloomer, S.H. 1992, Subduction zone infancy: Examples from the Eocene Izu-Bonin-Mariana and Jurassic California: Geological Society of America Bulletin, v. 104, p. 1621–1636.

Stinton, J.M., and Detrick, R.S., 1992, Mid-ocean ridge magma chambers: Journal of Geophysical Research, v. 97, p. 197–216.

Stix, J., Kennedy, B., Hannington, M., Gibson, H., Fiske, R., Mueller, W., and Franklin, J., 2003, Caldera-forming processes and the origin of submarine volcanogenic massive sulfide deposits: Geology, v. 31, p. 375–378.

Stuben, D., Neumann, T., Taibi, N.E., and Glasby, G.P., 1995, Variations in hydrothermal activity at the Mariana arc backarc spreading center at 18°13'N between 1987 and 1990: Chemie der Erde, v. 55, p. 61–79.

Taylor, B., Klaus, A., Brown, G.R., and Moore, G.F., 1991, Structural development of Sumisu Rift, Izu-Bonin arc: Journal of Geophysical Research, v. 96, p. 16,113–16,129.

Taylor, R.N., Murton, B.J., and Nesbitt, R.W., 1992, Chemical transects across intra-oceanic arcs: Implications for tectonic setting of ophiolites, *in* Parson, L.M., Murton, B.J., and Browning, P., eds., Ophiolites and their modern oceanic analogues: Geological Society of London, Special Publication 60, p. 117–132.

Tamura, Y., Gill, J.B., Tollstrup, D., Kawabata, H., Shukuno, H., Chnag, Q., Miyazaki, T., Takahashi, T., Hirahara, Y., Kodaira, S., Ishizuka, O., Suzuki, T., Kido, Y., Fiske, R.S., and Tatsumi, Y., 2009, Silicic magmas in the Izu-Bonin oceanic arc and implications for crustal evolution: Journal of Petrology, v. 50, p. 685–723.

Tegart, P., Allen, G., and Carstensen, A., 2000, Regional setting, stratigraphy, alteration and mineralization of the Tambo Grande VMS district, Piura Department, northern Peru, *in* Sherlock, R.L., and Logan, M.A.V., eds., Volcanogenic massive sulphide deposits of Latin America: Geological Association of Canada, Mineral Deposits Division, Special Publication 2, p. 375–405.

Titley, S.R., 1993, Relationship of stratabound ores with tectonic cycles of the Phanerozoic and Proterozoic: Precambrian Research, v. 61, p. 295–322.

Tivey, M.A., and Johnson, H.P., 2002, Crustal magnetization reveals subsurface structure of Juan de Fuca Ridge hydrothermal vent fields: Geology, v. 30, p. 979–982.

Viereck, L.G., Flower, M.F.J., Hertogen, J., Scmincke, H.-U., and Jenner, G.A., 1989, The genesis and significance of N-MORB sub-types: Contributions to Mineralogy and Petrology, v. 102, p. 112–126.

Walker, P.N., and Barbour, D.M., 1981, Geology of the Buchans ore horizon breccias, *in* Swanson, E.A., Strong, D.F., and Thurlow, J.G., eds., The Buchans orebodies—Fifty years of geology and mining: Geological Association of Canada Special Paper 22, p. 161–185.

Wohletz, K., and Heiken, G., 1992, Volcanology and geothermal energy: Berkeley, University of California Press, 432 p.

Wright, I.C., Stoffers, P., Hannington, M., de Ronde, C.E.J., Herzig, P., Smith, I.E.M., and Browne, P.R.L., 2002 Towed-camera investigations of shallow-intermediate water-depth submarine basaltic stratavolcanoes of the southern Kermadec arc, New Zealand: Marine Geology, v. 185, p. 207–218.

Yang, K., and Scott, S.D., 1996, Possible contribution of a metal-rich magmatic fluid to a seafloor hydrothermal system: Nature, v. 383, p. 420–423.

Yang, K., and Scott, S.D., 2006, Magmatic fluids as a source of metals in seafloor hydrothermal systems, *in* Christie, D.M., Fisher, C.R., Lee, S-M, and Givens, S., eds., Back-arc spreading systems—Geological, biological, chemical, and physical interactions: American Geophysical Union Geophysical Monograph 166, p. 163–184.

Yuasa, M., and Kano, K., 2003, Submarine silicic calderas on the northern Shichito-Iwojima Ridge, Izu-Ogasawara (Bonin) arc, Western Pacific, *in* White, J.D.L., Smellie, J.L., and Clague, D.A., eds., Explosive subaqueous volcanism: American Geophysical Union, Geophysical Monograph 140, p. 231–243.

Zierenberg, R.A., Shanks, W.C., III, Seyfried, W.E., Jr., Koski, R.A., and Strickler, M.D., 1988, Mineralization, alteration, and hydrothermal metamorphism of the ophiolite-hosted Turner-Albright sulfide deposit, southwestern Oregon: Journal of Geophysical Research., v. 93, p. 4657–4674.